# Preprints.org

Article

# Emergence and progression of behavioral motor deficits and skeletal muscle atrophy across adult lifespan of the rat

Max GrönholdtKlein , Ali Gorzi , Ling Wang , Erik Edström , Eric Rullman , Mikael Altun , Brun Ulfhake [*]

*Article*

# Emergence and Progression of Behavioral Motor Deficits and Skeletal Muscle Atrophy across Adult Lifespan of the Rat

**GrönholdtKlein, M. [1,†], Gorzi, A. [2,†], Wang, L. [3,†], Edström, E. [4], Rullman, E. [5], Altun, M. [5,§] and Ulfhake, B. [5,*,§]**

[1]   Department of Neuroscience, Karolinska Institutet, Sweden; maxgronholdtklein@gmail.com
[2]   University of Zanjan, Zanjan, IRAN; ali_gorzi@znu.ac.ir
[3]   School of Medicine, Inner Mongolia Minzu University, Inner Mongolia, P.R.C.; wlzh001@aliyun.com
[4]   Department of Clinical Neuroscience, Karolinska Institutet, Sweden; erik.edstrom.1@ki.se
[5]   Department of Laboratory medicine, Karolinska Institutet, Sweden; eric.rullman@ki.se (R.E.); mikael.altun@ki.se (A.M.)
[*]   Correspondence: brun.ulfhake@ki.se
[†]  Shared first author.
[§]  Shared last authors.

**Abstract:** The facultative loss of muscle mass and function during aging (sarcopenia) poses a serious threat to our independence and health. Much of what we know about sarcopenia derive from studies on small rodents which serve as models for the human condition. Here we used outbred male rats to study the natural history of sarcopenia with the aim to compare behavioral motor deficits with degree of muscle wasting and to find processes underlying the preclinical phase of sarcopenia. Selected metrics were validated in female rats. We used the soleus muscle because of its long duty cycles in everyday life and significance for postural control. The results show that gait and coordination remain intact through middle age (12-18 months; 40%-60% of median lifespan) when muscle mass relative to body weight is largely maintained. The muscle, however, show multiple signs of remodeling with a shift in myofiber-type composition towards type I, increased number of hybrid fibers and fibers expressing embryonic myosin. In parallel with the shift in fiber type prevalence, fiber type clustering increased. The latter combined with a transcriptional upregulation of nicotinic acetylcholine receptor subunit γ (CHRNγ ), NCAM and Myogenin (MYOG) suggests a remodeling driven by myofiber denervation. Additional stigmata were increased number of central nuclei, transcriptional upregulation of Smad3, FBXO32, and MuRF1mRNAs; unaltered density of satellite cells (SC) and βCatenin mRNA. In early (25-month-old) and advanced (30-month-old) aging, gait and coordination deteriorate as loss of muscle mass progresses. In late middle age and early aging because of a type II atrophy (>50%), followed by type I atrophy (>50%). Number of myofiber did not correlate with this process. At advance age, the atrophy is accompanied by a decrease in SC and βCatenin mRNA while several transcripts upregulated earlier-on were downregulated. In contrast, glial-derived nerve growth factor (GDNF) mRNA abundance peaked at endpoint. We conclude that sarcopenia in the rat as in humans, has a long preclinical phase where the muscle undergoes extensive remodeling to preserve muscle mass and function. The data supports the notion that myofiber denervation is the instigating mechanism, initially affecting large type II motor units (MUs) and at more advanced stage also the smaller type I MUs.

**Keywords:** ageing; sarcopenia; dynapenia; skeletal muscle atrophy; denervation; behavior

## Introduction

In the middle age and beyond, we experience that the speed, strength, and mass of our muscles dissipates. This facultative loss of muscle mass and function (sarcopenia) poses a serious threat to our independence and health at older age. Sarcopenia was recognized by WHO[1] in 2002 as a condition in elderly people associated with a range of morbidities and is now a disease entity with ICD-10-CM code (M62.84). Guide-lines for diagnostic criteria have been assembled and revised by European, Asian and North American work groups (the EWGSOP2[2,3], the Asian Working Group for Sarcopenia (AWGS)[4], and the FNIH[5]) and define primary sarcopenia as a loss of skeletal muscle mass, decrease in muscle strength (static handgrip strength) and motor performance (usually gait speed). Sarcopenia becomes a clinical condition at 60-to-70 years-of-age (i.e. early aging) and later sarcopenia may be the prime cause for disability [6]. However, studies indicate a decline in muscle function already in the transition between young adulthood and early middle age [7–13], suggesting that sarcopenia may evolve from processes instigated early-on and when becoming clinically overt been ongoing for decades.

Much of what we know about sarcopenia derive from studies on laboratory rodents which serve as models for the human condition (reviewed in[8,14–18]). As concluded by Ballak et al, rats seem to mirror the human condition more closely than mice do[15], while mice offer a more flexible platform for genetic manipulations. Aged skeletal muscles of rodents [18–33] and humans[34–42], consistently show loss and atrophy of fast-twitch type II myofibers [43]. In parallel, there is a decline in satellite cells (SC, stem cells for replenishment/ expansion of the muscle pool of myocytes) and a decrease in SC replication rate [at least in vitro][44,45]. The aged skeletal muscle also shows signs of inflammation, accumulation of extracellular matrix components, and intra and inter myofiber infiltration of fat (*idem*). The combined effect of these changes is mirrored in the loss of muscle mass and function at old age. Among factors proposed to be driving these changes are the accumulation in the muscle of senescent cells and their secretome, systemic alteration in inflammatory and endocrine signalling, age-associated changes in the cellular balance between synthesis and breakdown of proteins along with changes to nutritional balance and gut microbiota, and a more sedentary life-style of the elderly [laboratory] rodents and humans alike(*idem* and [33,46–49]).

The vulnerability of fast-twitch type II myofibers, occurrence of fibre type grouping[17,29,40] and fragmentation and irregularities of the post synaptic junctional membrane[50] suggest a neurogenic component in sarcopenia. This is further supported by the increasing number of fibres with a myosin expression pattern intermediate of type I and type II (hybrid fibres), alterations of the chemical phenotype of motoneurons [51], changes to excitability and impulse propagation changes, as well as a loss of MUs and a compensatory enlargement of the remaining MUs [15,17,52–57]. If a neurogenic component precedes, is concurrent with, or a consequence of changes intrinsic to the skeletal muscle, remains a debated controversy [8,16–18,31,32,50,57–62], since cause-and-effect is hard to pin down due to the multitude of changes present in sarcopenic muscles.

In this study, we have used outbred rats to study the natural history of sarcopenia with the aim to compare behavioral motor deficits with degree of muscle wasting and to find processes preceding the clinical phase of this condition. For these purposes we used the soleus component of the triceps surae muscle of male SD rats because of its long duty cycles in everyday life and significance for postural mechanisms[63]. In addition, select metrics were validated also in young adult, middle-aged and aged female rats.

## Material and Methods

### *Study population*

Although the main focus of this work is on male Sprague Dawley rats, rats of both sexes were used and delivered by (Scanbur, Sollentuna, Sweden; Charles River, Dortmund, Germany) being ~8 weeks old (Table 1). In the vivarium, the rats were housed in macrolon cages (type 4, lid type 4) with aspen chips as bedding, kept 4-5 per cage with a holding room temperature of $21 \pm 2\,^{\circ}C$ and 40-60% humidity, and a 12h light-dark (LD) cycle. The rats had ad libitum access to rodent feed (R70,

Lactamin) and weakly chlorinated water, refreshed weekly. Environmental enrichment was provided with plastic tubes and chew-sticks. Health inventories at the facility were conducted in accordance with FELASAs recommendation and besides Helicobacter pylori not included in the testing panel), the animals were free of pathogens named on the FELASA exclusion list. Prior to experiments, the rats were acclimatized for approximately two weeks. Welfare checks were executed by trained technicians under the supervision of the designated veterinarian.

**Table 1.**

| Cohort | Sex | Age (months) | Strain | Vendor | Cage type | Temp °C | Humidity (%) | Feed | n |
|--------|-----|--------------|--------|--------|-----------|---------|--------------|------|---|
| M5m | Male | 5 | CR-SD* | CR | Type 4 Open | 21±2 | 40-60 | Lactamin R70 | 10 |
| M12m | Male | 12 | CR-SD* | CR | Type 4 Open | 21±2 | 40-60 | Lactamin R70 | 9 |
| M18m | Male | 18 | CR-SD* | CR | Type 4 Open | 21±2 | 40-60 | Lactamin R70 | 11 |
| M25m | Male | 25 | CR-SD* | CR | Type 4 Open | 21±2 | 40-60 | Lactamin R70 | 8 |
| M30m | Male | 30 | Sprague-Dawley | Scanbur | Type 4 Open | 21±2 | 40-60 | Lactamin R70 | 16 |
| F3m&F3mA | Female | 3 | Sprague-Dawley | Scanbur | Type 4 Open | 21±2 | 40-60 | Lactamin R70 | 30 |
| F12m | Female | 12 | Sprague-Dawley | Scanbur | Type 4 Open | 21±2 | 40-60 | Lactamin R70 | 10 |
| F30m | Female | 30 | Sprague-Dawley | Scanbur | Type 4 Open | 21±2 | 40-60 | Lactamin R70 | 10 |
| Total | Males | | | | | | | | 55 |
| Total | Females | | | | | | | | 50 |

Based on the outcome of behavioral testing and gross metrics see below, a group of 18-month-old males was added and substituted for the 12-month-old male rats in the muscle histology and gene expression analyses of this study.

The use of laboratory rats and all experimental procedures were agreed upon, reviewed, and approved by the regional Laboratory Animal Ethics Council (Stockholms Djurförsöksetiska nämnd; project licenses N122/03, N122-N124/06).

*Behavioral testing*

Animals of both sexes were subjected to a standardized set of behavioral tests according to a previously published protocol[64] at an age of 3 months (female rats), 5 months (male rats), 12 months (female and male rats), 25 months (male rats) and at study endpoint (30 months, male and female rats) (Table 2). Briefly, the test battery included:

*Open field activity.* Explorative behavior was studied in a square area with walls (70×70×30 cm) in gray colored plastic. For 3 minutes the movement distance, number of rearings and number of grooming behaviors were recorded

*Crossing a wire mesh screen.* A 70 cm long, 2.5 cm-wire mesh screen was used to record time-to-pass and number of limb placement errors.

*Beam balance.* A 2.5 cm-wide wooden beam suspended 50 cm above a soft surface. The rat was placed on the beam for a maximum of 60 s. Time on beam was recorded and performance was ranked according to [65]. The test was repeated three times and the mean outcome was taken as the result of the test.

*Walking track analysis*. The animals' feet were stained with non-toxic acrylic paint (fore paws with red and hind paws with black color), and they then had to walk through an 8.5×42 cm transparent Plexiglas tunnel with the "home cage" as "attractor" at the other end. The walking tracks were used to estimate (a) stride length (distance between fore paw-fore paw and hind paw-hind paw) and (b) gait width (distance between left and right hind paws) as previously described (*idem*).

*Gait score*. We followed the protocol described in detail in [64]. Briefly, the scoring is based on assessment the limbs body weight bearing capacity (from 0=walk/stand on digits; up to 3=fail to raise the body trunk completely from the supportive surface) and if each limb shows a complete gait cycle (stance, paw-off, swing, paw-on) coordinated with the other limb(s). Scoring 0=all phases of the gait cycle present and movement coordinated with the other limbs; 3= gait cycle phases missing and not coordinated). Gait score 0= no signs of dysfunction, 1= mild or infrequent errors, 2= regular gait errors/insufficient weight bearing support, and 3 = severe gait dysfunction. Gait scoring was executed on all rats included in this study (Table 2).

**Table 2.**

| Cohort | Sex | Age (months) | Behavioural tests | | Mesh crossing | Gait | Gait-stage | Gross measures | | SI |
| | | | OF | Beam balance | | | | BW | m. sol weight | |
|---|---|---|---|---|---|---|---|---|---|---|
| M5m | Male | 5 | X | X | X | X | X | X | X | X |
| M12m | Male | 12 | X | X | X | X | X | X | X | X |
| M18m | Male | 18 | ND | ND | ND | ND | X | X | X | X |
| M25m | Male | 25 | X | X | X | ND | X | X | X | X |
| M30m | Male | 30 | X | X | X | X | X | X | X | X |
| F3m | Female | 3 | X | X | X | X | X | X* | X* | X* |
| F12m | Female | 12 | X | X | X | X | X | X* | X* | X* |
| F30m | Female | 30 | X | X | X | X | X | X* | X* | X* |

\* data replotted from Edstrom et al., 2008

*Experimental endpoint*

The animals were humanely euthanized at 3-, 5-, 12-, 18-, 25-, and 30-months by an overdose of pentobarbital sodium and during the terminal anesthesia the components of the triceps surae muscle were quickly harvested. The fresh tissue was weighed, snap frozen in liquid nitrogen chilled iso-pentane, and stored at -80°C until further use.

**Histology**

*Counting of myofibers and myonuclei with a central position*

We followed our previously published protocol[66](see also Supportive information for details). From male rats the soleus muscle in young adult (5-month-old), middle aged (18-month-old), early aged (25-month-old), and advanced aged (30-month-old, endpoint) were transversely sectioned distal to muscle origin (i.e. the portion of the muscle belly that should hold all myofibers of the soleus muscle) into series of 8 or 10 µm thick sections in a cryostat, and thawed onto gelatin-coated slides. The sections were stained with hematoxylin and eosin (EosinHTX) according to a standard protocol (see Supplementary information). The stained tissue sections mounted on coded slides were examined with a Nikon Optiphot (x10/0,45 dry planApo objective). Images were captured with a Hamamatsu C8484-05G digital camera. The photos were composited to pictures covering the whole muscle cross-section in Adobe Photoshop CSS 12.1x64 or ImageJ (version 1.45S). The pictures were

opened in ImageJ, and the total number of fibers and number of fibers with central nuclei (CN)were recorded using the Cell Counter plug-in of ImageJ. Slide codes were disclosed after counting had finished.

*Immunohistochemistry*

Adjacent or near adjacent 8 μm thick sections prepared in the section series described above were dried in RT for 30 min. A well was created using a DAKO pen. The tissue was then fixated in 4% formaldehyde for 10 minutes then rinsed in cold tap water for 10 minutes repeated three times. Epitopes were blocked with 5% normal donkey serum for one hour in RT. Primary antibodies towards embryonic (MyHCe/MyHC3; moAb, DSHB), slow (MyHCs, type I, moAb Novocastra) and fast (MyHCf, type II, moAb Novocastra) were incubated for either 1h at 37°C or overnight at 4°C (see Supportive information). Following incubation with the primary antibody and repeated washing, the sections were incubated with a secondary antibody for one hour at RT and kept away from exposure to light. After washing the sections were mounted with DAPI and cover slipped. Sections were then stored at 4-8 °C before imaging.

For counting of nuclei presumed to be satellite cells, DAPI (Vector lab) was used as unspecific marker of nuclei. Primary antibodies (sequential labeling for each epitope) were either directed toward Pax7 (DS Hybridoma Bank; see Supportive information) and Laminin (The Binding Site or Sigma; see Supportive information), or against Pax7 and Ki67 (Novocastra, Supportive information). Following repeated washing, the sections were incubated with a mixture of secondary antibodies raised in donkey against respective species of the primary antibody and processed as described above. Imaging was captured with LSM700 confocal laser scanning microscope (Carl Zeiss), for details see Supportive information.

*Fiber typing and stereology*

Images for fiber typing was acquired on a Zeiss LSM700 confocal laser-scanning microscope. Images were processed using ZEN2012 software (Zeiss) (further details in Supportive information). Multi-panel figures were assembled using Adobe Photoshop CS6 software (Adobe Systems). The analyses were performed on composite microimages as described above. The person analyzing the images was blinded to the experimental group. Three adjacent or near adjacent sections from each rat were used, one marked for slow myosin (MyHC I), another for fast myosin (MyHC II) and a third for embryonic myosin (MyHC3). By tracing across adjacent sections, myofibers were categorized as being type I (only immunoreactive (IR) to slow myosin), type II expressing fast myosin IR only, hybrid fiber expressing both slow and fast myosin IRs, and myofibers expressing the embryonic isoform of myosin (MyHC III/MyHC3). MyHC-III colocalized with either one or both slow and fast myosin isoforms, i.e., type-I, type-II and hybrid fibres Software ImageJ was used for data collection.

Using a grid-mesh casted over the section stained for slow myosin, the muscle section was divided into subregions (grid boxes of 300k pixels size each; see Supportive Information and Figure S1) for analysis by unbiased systematic sampling (stereology). Only fibers that did not touch the cell borders or only touched the left or the top sides of each square were systematically counted (Figure S2, green dots). A starting grid box was selected using a random number generator and every 15th consecutive grid box was counted until a minimum of 200 fibers per muscle was registered and mapped to immunoreactivity for one or several of MyHC3, MyHC I and MyHC II in the adjacent sections. In cases where the regional tissue quality was compromised, the counting grid was moved six squares ahead until a grid box enabling analysis was reached.

Fiber type enclosure (fibre-type grouping, fibre-type clustering; [35]) was examined for type I fibers using the same stereological approach as described above and following the protocol described in [67]. This included assessment of number of neighbor (n) fibers in each age group to determine the probability $NP^{(n+1)}$ of fiber enclosure, where N is the assessed prevalence of the fiber type in each age cohort. $NP^{(n+1)}$ is used to calculate the frequency of enclosed fibers by a random distribution based on assessed prevalence and number of neighboring fibres (*idem*).

Counting of nuclei being Pax7-IR immediately adjacent to a myofiber and within the laminin boundaries (≥117 myofibers per case) was done on single sections by multicolor imaging as described in Supportive information. We used the same method to decide on colocalization of Pax7-IR and KI67-IR. Ki67 was used as marker for replicating Pax7-IR profiles[68].

Further, several sections from each group used to count number of fibers, number of myonuclear profiles, central nuclei, expression of different MyHC immunoreactivities and fiber CSA were subjected to independent validation by a second examiner and the results were generally in very close agreement (<5%) and differed never by more than 10% between operators.

Tables 1–3

**Table 3.**

| Cohort | Sex | Age* (months) | Muscle histology analyses | | CSA | CN | SC number | SC replication |
| | | | Fiber number | Fiber types | | | | |
|---|---|---|---|---|---|---|---|---|
| M5m | Male | 5 | X | X | X | X | X | X |
| M18m | Male | 18 | X | X | X | X | X | X |
| M25m | Male | 25 | X | X | X | X | X | X |
| M30m | Male | 30 | X | X | X | X | X | X |
| * age when included in study | | | | | | | | |

*RNA extraction and qPCR*

Total RNA was prepared by the Trizol method (Invitrogen, Life Technologies) using a drill knife and quantified spectrophotometrically by absorbance at 260 and 280 nm with PicoDrop (Picopet01, Picodrop Ltd, Cambridge UK). Reverse transcriptions were performed with Applied Biosystems High-Capacity cDNA Reverse Transcription Kit as described in detail in the Supportive information.

Primers were designed using the NCBI software Primer-BLAST (for nucleotide sequence and accession number see Supportive information) and gene transcripts analyzed here were selected based on earlier studies on aging rats[69,70], response to axonal damage and regeneration in rats [66], and early and advanced aged muscles in humans[71]. Amplicons by qPCR were controlled with respect to length and number of products with melt curve as well as agarose gel electrophoresis using ethidium bromide as stain. For details on PCR-reaction see protocol in supplemented information. CT-values for each individual were then normalized (ΔCT) with the endogenous control gluthathionperoxidase-1 or β-Actin[70,72]. Correction for intra-experimental-efficiency was conducted using a carry-over triplicate on each plate from an aliquoted cDNA-pool for identical freeze-thaw-cycles.

*Surgical intervention*

Female rats were subjected to a sciatic axotomy (n=10 and n=10 served as controls; Table 1) under general anesthesia at an age of 3 months. All surgical procedures were carried out in an aseptic manner. An incision was made on the posterior aspect of the right thigh, the sciatic nerve was identified just below the ramification of the posterior biceps-semitendinosus branch where the nerve was transected with a sharp knife and ligated (to prevent outgrowth). Recovery from anesthesia on a heat pad at 37°C until awake and moving, usually 3-4 h. Recovery from surgery was given 4-5 days after which behavioral examination was performed to assess the loss of function. Only animals that had lost their ability to stand/walk on their right hind limb paws (toes/digits) were included in the

study. Following 10 days survival, the animals were euthanized, and relevant tissues snap frozen for further PCR analysis.

*Statistical analyses and models*

Analyses of variance were conducted either with Kruskal-Wallis analysis of variance (nonparametric testing) or ANOVA (parametric testing) with post hoc pairwise testing (multiple pairwise testing according to the Steel-Dwass-Critchlow-Fligner method) or Bonferroni post hoc testing, using either the Statistica® software package 6.1 (Statsoft, Tulsa, OK, USA) or the XLSTAT® add-on software for MS Excel. Cox-Mantel test was used to explore differences in survival rate. P-value of <0.05 was considered significant. Principal Component Analysis (PCA) was performed on R version 3.3.3 or XLSTAT. PCA was used to (1) explore correlations between metrics of spontaneous activity, motor and reflex functions, histological variables, and gene expression data of the different age cohorts and to (2) visualize the impact by age and sex on motor-and-coordination-functions (males and females, and on gene-expression and histological data (only males).

## Results

*Survival and gross observations*

The median survival age of the female (~30.5 month) and male (~29.3 month) rats studied until the endpoint was not significantly different (p=0.83; Figure 1). Both female and male rats increase in body weight through young adulthood and middle age (Table 4), female rats with ~131% (12-month-old) while males gained ~230% until 18-months of age. In parallel, there was an increase in skeletal muscle mass that matched (~135%, 12-month-old females), or nearly matched (~200%, 18-month-old males), the change in whole body weight (Table 4; see also Supportive information Figure S3). Thus, the relative muscle mass, normalized m. soleus muscle mass (muscle weight/whole body weight, mg/g, [29,73]) remained largely unchanged from young adulthood into early middle age. During late middle age (18-month-old) and early aging (25-month-old) there is a gradual drop in normalized muscle mass which becomes accentuated in advanced age (30-month-old) causing a significant decrease in both sexes (Table 4). During early aging, the loss of skeletal muscle mass is paralleled by the emergence of behavioural gait disturbances evident in some but not all subjects (Figure 2; detailed box plots with pairwise statistical testing is available in Supportive information (Figure S3)). As aging progresses, the drop in normalized soleus mass, gait and coordination deteriorate (Figure 2). There was a close correlation ($r^2 \geq 0.75$; p<0.001) between gait score (see Material and methods), normalized soleus mass, and age in female and male rats across adult lifespan (Figure 2B).

**Table 4.**

| Cohort | Sex | | Age (months) | Body weight (g) | M. soleus wet weight (mg) | Norm sol wet weight (mg/g) | Gait score |
|--------|-----|------|------|------|------|------|------|
| M5m | Male | mean | 5 | 359.4 | 175.8 | 0.490 | 0 |
| | | ±SD | | 23.8 | 13.0 | 0.040 | 0 |
| | | n | | | 10 | | |
| M18m | Male | mean | 18 | 819.9 | 348.0 | 0.43 | 0 |
| | | ±SD | | 124.0 | 52.0 | 0.031 | 0 |
| | | n | | | 11 | | |
| M25m | Male | mean | 25 | 802.3 | 315.6 | 0.41 | 1.3 |
| | | ±SD | | 155.0 | 50.6 | 0.11 | 0.5 |
| | | n | | | 9 | | |
| M30m | Male | mean | 30 | 502.5 | 98.5 | 0.19 | 2.6 |
| | | ±SD | | 52.9 | 27.4 | 0.043 | 0.5 |
| | | n | | | 16 | | |
| F3m* | Female | mean | 3 | 266.1 | 128.3 | 0.48 | 0 |

|  |  |  |  |  |  |  |  |
|---|---|---|---|---|---|---|---|
|  |  | ±SD |  | 8.6 | 6.5 | 0.020 | 0 |
|  |  | n |  |  | 10 |  |  |
| F12m* | Female | mean | 12 | 348.3 | 174.4 | 0.49 | 0 |
|  |  | ±SD |  | 30.2 | 27.2 | 0.044 | 0 |
|  |  | n |  |  | 10 |  |  |
| F30m* | Female | mean | 30 | 338.1 | 71.7 | 0.22 | 2.1 |
|  |  | ±SD |  | 38.4 | 16.9 | 0.035 | 0.7 |
|  |  | n |  |  | 10 |  |  |
| Kruskal-Wallis | Males | p= | <0.001 | <0.001 | <0.001 | <0.001 |  |
| Kruskal-Wallis | Females | p= | <0.001 | <0.001 | <0.001 | <0.001 |  |

\* data replotted from Edström et al., 2008
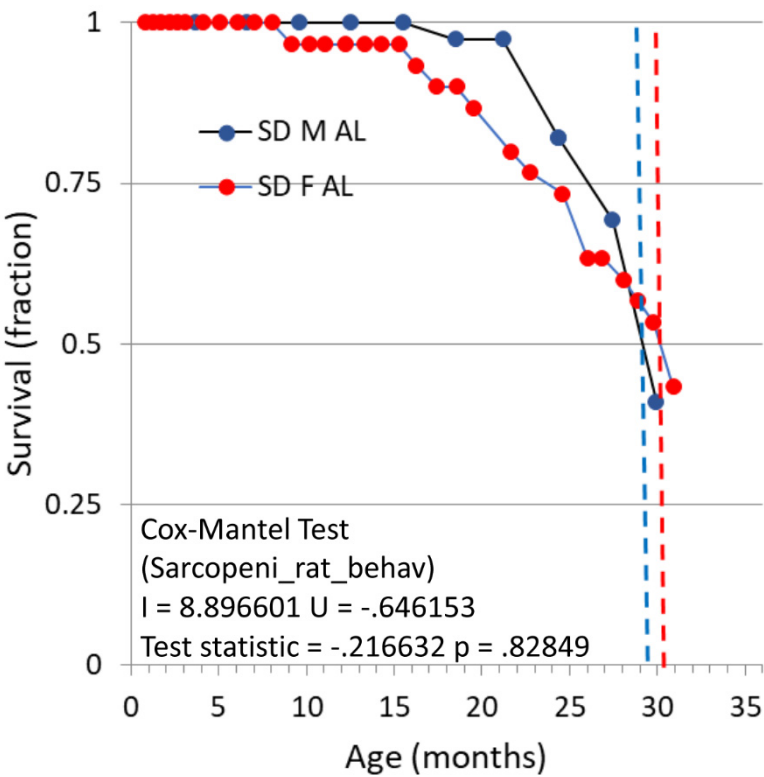


**Figure 1.** Survival of female (red) and male (blue) for cohorts of rats maintained until they reached the median survival age (endpoint of this study). The difference between males and females was not significant (Cox-Mantel test).
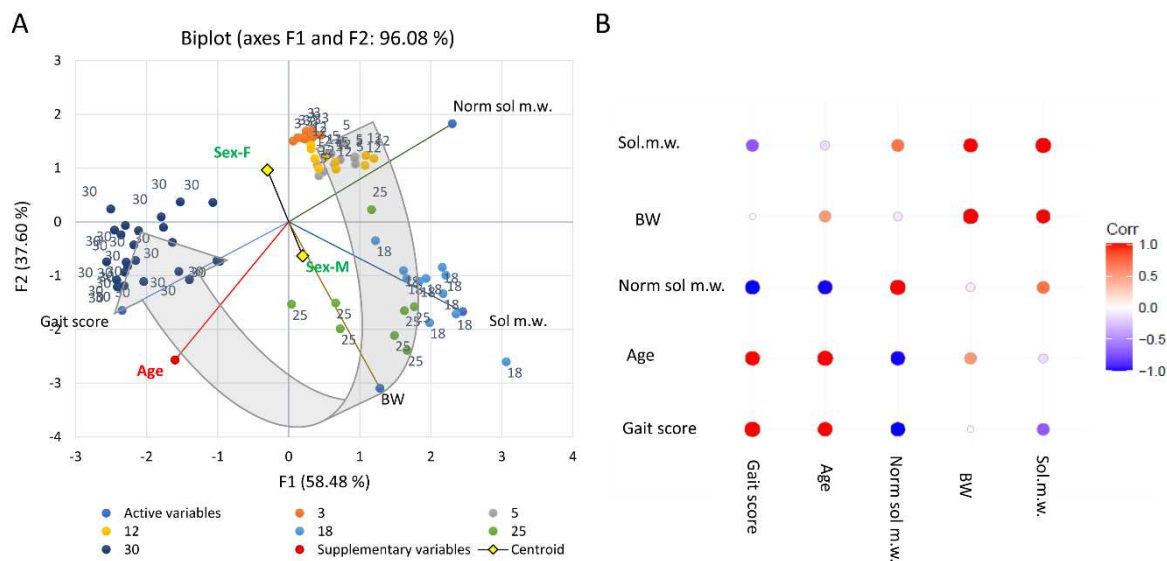
**Figure 2.** (A) PCA analysis of gross metrics on male (5-, 18-, 25- and 30-month-old) and female (3-, 12- and 30-month-old) rats show covariance with 96% of the total variance explained by the two first principal components (F1 and F2). Note that age is a supplementary variable not contributing to the factor loading on the F1 and F2 axes. As the inserted arrow indicates, male rats in late middle age (18-month-old) and early aging (25-month-old) separate from young adults (male and female, 3- and 5-month-old) and females in the early middle age (12-month-old) mainly along F2, driven by their larger body and muscle weights and the incipient drop in normalized soleus muscle weight. In advanced age (30-month-old) male and female rats separate from the other age groups mainly on the F1 axis driven by gait deterioration and progressive muscle atrophy. Young-adult males and females and early middle-aged-females group tightly together. The sex mixed group at advanced age (30-month-old) form rather dense clusters while the observations in males at late middle age (18 month-old) and in early aging (25-month-old) are scattered. There is a sex difference (centroids) driven by differences in whole body size and muscle weight. (B) Correlation coefficients between metrics have been colour coded with shades of red denoting positive correlations while shades of blue indicate an inverse correlation.

Table 4

*Emergence of behavioural motor impairments of aging rats*

We used a battery of behavioural tests[64,74] to assess changes in motor performance and coordination across the adult lifespan of male and female rats (3 and 5-, 12- and 30 months old rats) but also alterations in level of spontaneous activity displayed in the open field test (see Material and methods). As indicated in Figure 3 (A-C), we found strong covariations among these behavioural indicis and only a minor difference between the sexes (*idem*). The observations in early aged male rats (25 month) were positioned in between the observations of 12-month-old and 30-month-old female and male rats (See supportive information (Figure S4)).
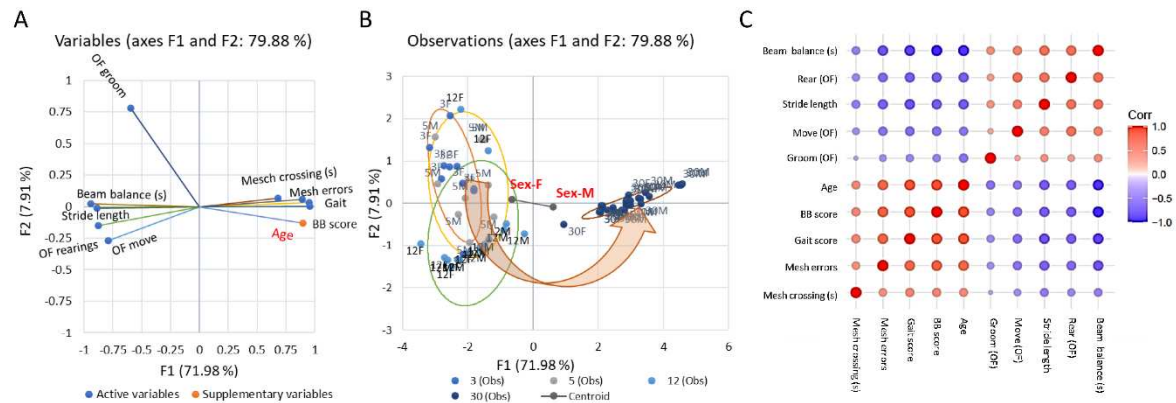
**Figure 3.** (A) PCA analysis of activity, motor, and coordination indicis in male and female age cohorts (3-, 5-, 12- and 30-month-old) show high degree of covariance with 80% of the total variance explained by the two first principal components (F1 and F2). Note that age is a supplementary variable not contributing to the factor loading on the F1 and F2 axes. Motor and coordination indicis loaded mainly on F1 being directly or inversely mutually correlated. (B) Young adult female and male rat observations overlap extensively as do the male and female observations in early middle age, while the observations on middle aged rats of both sexes are slightly shifted away from the young adults on the F2 axis driven by changes of the activity indices in the OF test and shorter time on the BB. At advanced age, the observations are significantly separated from both young adult and middle-aged rats along the F1 axis because of the deterioration of motor and coordination capacities. There is a sex difference (centroids connected with a line) driven by middle and advanced aged female rats performing somewhat better than their male counterparts. Observations on early aged males (25-month-old) not included in the comparison of both sexes formed a group positioned in between middle aged and 30-month-old rats (see Supportive information (Figure S4)). (C) Correlation coefficients between metrics in A have been colour coded with shades of red denoting positive correlations while shades of blue indicate an inverse correlation.

In both sexes, all behavioural metrics showed significant changes across the adult lifespan (K-W $p<0.03$ to $p<0.0001$; for age-wise comparison within sexes see the Supportive information (Figure S5)). The gait indices (score, stride length, stride width) and normalized soleus mass were closely intercorrelated (fraction of explained variance >75%; Figure 4).
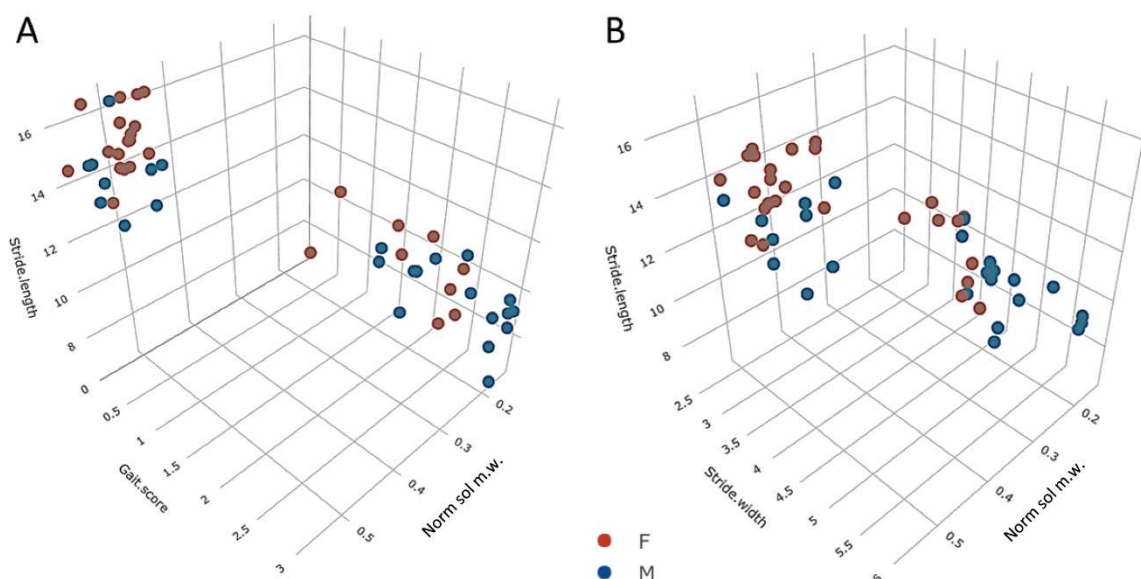
**Figure 4.** Three-axis plots of the covariation between normalized soleus mass, on the one hand, and (A) stride length and gait score, and (B) stride width and stride length, on the other. Observations in males in blue and females in red. Multiple R(z/xy) for female and male rats were in (A) =0.89 (both sexes; p=1E-7) and in (B) r=0.88 (males, p=2E-7) and r=0.87 (females, p=1E-7).

*Number of myofibers, myofiber type composition, and myofiber cross sectional area of male rat m. soleus*

Histological examination across the adult lifespan revealed that aging associates with increased variability of myofiber shape and cross sectional area (CSA), and enlargement of the interstitial matrix space (Figure 5). M. soleus is a mixed muscle having myofibers predominantly immunoreactive (IR) to MyHC I (type I fibres, ~80% ) in the young adults complemented by a smaller number of MyHC II-IR myofibers (type II fibres) (Figures 6 and 7; see also Supporting information for images of the full cross section of the soleus muscle (Figure S5) and Table S3). In young adult rats, myofibers IR to developmental myosin (MyHC3) are rare (<1% in the young adult rats; Figures 6 and 7, Supportive information Table S3) and only few myofibers co-express both MyHC I- and MyHC II-IR (hybrid fibres; <1% in young adult rats; *idem*).
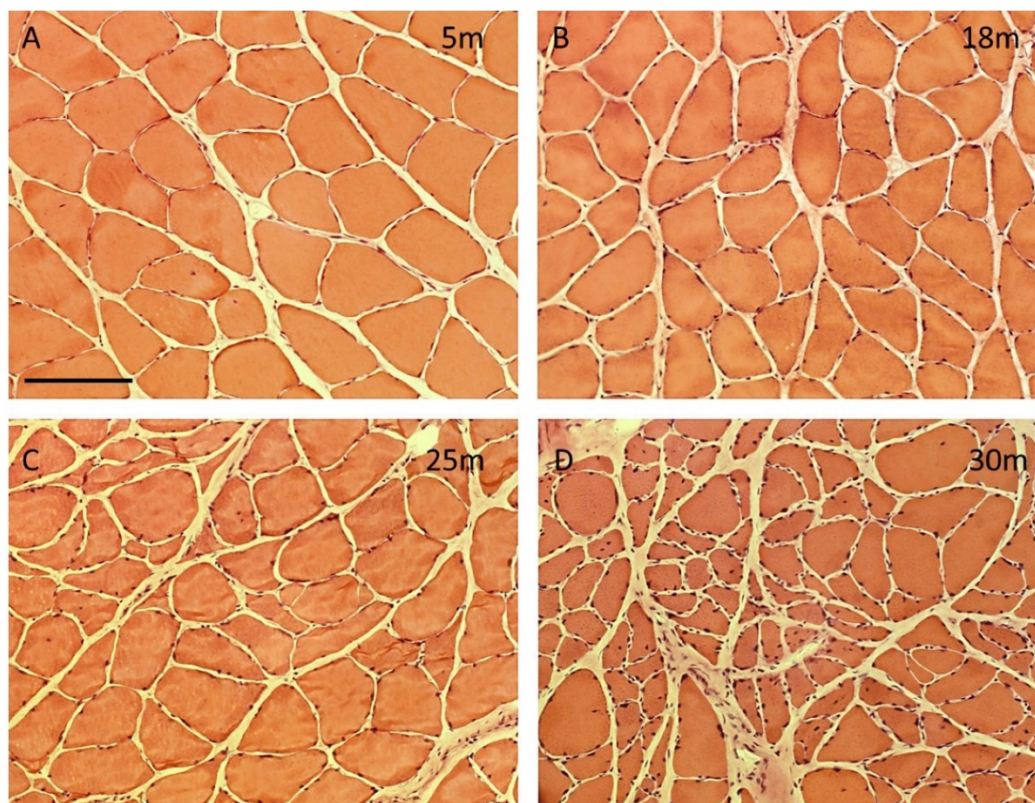


**Figure 5.** Cross sections of m soleus stained with Eosin-HTX from young adult (A), middle aged (B), early aged (C), and advanced aged (D) rats. With advancing age, the shape and size variability increases, as do the interstitial matrix space. Nuclei with a central position in the myofiber become more frequent during aging. (x10 plan-apo objective). Scale bar in A is 100µm and applies to all panels.
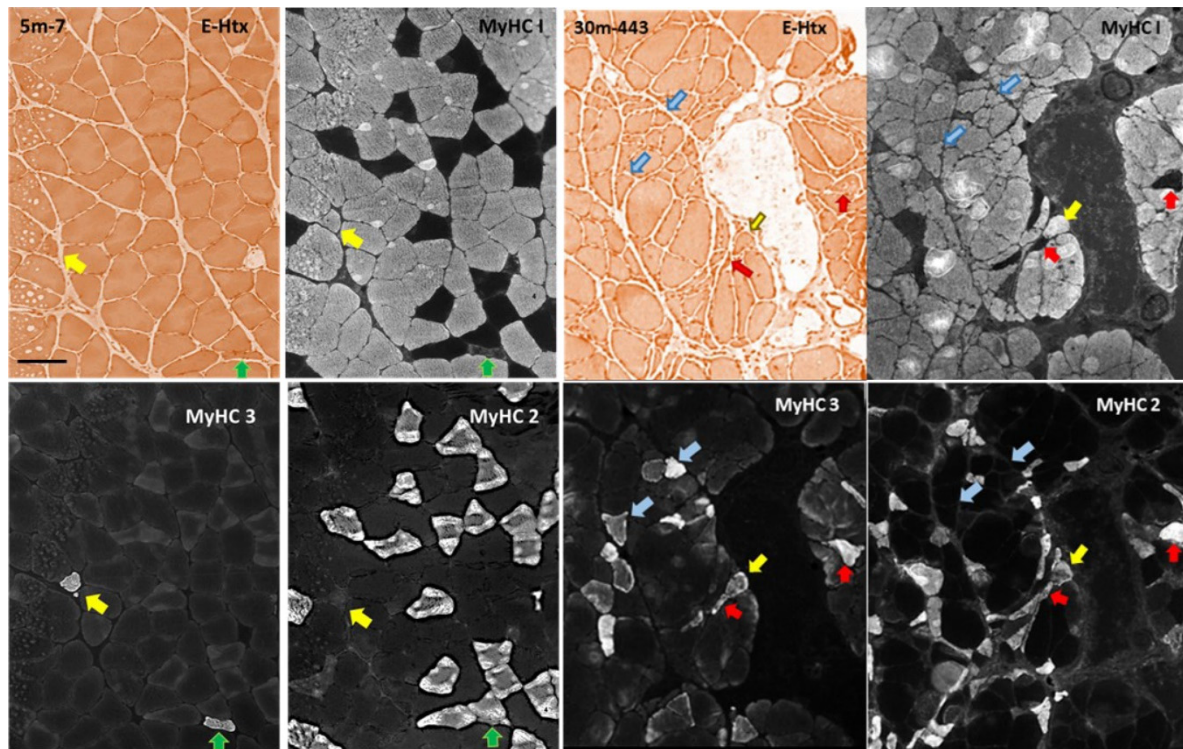
**Figure 6.** Series of near-adjacent sections from a young adult (5m-7; left four panels) and a rat at endpoint age (30m-433; four right panels) stained for Eosin-HTX, MyHC I-IR, yHC3-IR, and MyHC II-IR. In the panels of the young adult rat, a yellow arrow indicates a myofiber profile IR for MYHC I and MyHC3 but negative for MyHC II-IR. Green arrow points to a fine calibre fibre IR to MyHC II and 3, and faintly positive for MyHC I. In the panels to the right, the aged rat displays examples of myofibers IR for all three myosins (yellow arrow), IR to MyHC I and MyHC3 (blue arrows), and IR for MyHC II and MyHC3 (red arrows). Also note the high degree of shape variability among aged myofibers. The full m. soleus cross section from which the cut-outs used here to illustrate the changes imposed by aging is available in Supportive information (Figure S6). (x10 plan-apo objective), scale bar in upper left panel is 100 μm and applies to all panels.

In late middle age and prior to any overt behavioural deficit, type II fibres decrease in number with a parallel increase in type I and hybrid fibres (5%-10%) as well as fibres expressing MyHC3 (5%-10%; Figures 6 and 7). Also, type II cross sectional area (CSA) starts to drop while type I CSA is still well-preserved (*idem*). Later, at early and advance age when motor and coordination deficits are manifest (see above) some changes become more accentuated while other stigmata as myofibers expressing MyHC3 and frequency of hybrid fibres stay elevated at a rather constant level from late middle age and onwards (Figure 7). Towards the end of the lifespan, also type I fibres show a significant drop in CSA (>50%; Figure 7). The pattern of myosin co-expression changed with increasing age (Figure 8), where co-expression of myosin II and MyHC3 dropped substantially from 18 months until end point while hybrid fibres devoid of MyHC3 IR increased in parallel. Hybrid and myosin-I expressing fibres that also express MyHC3 increase from 18 to 25 month of age with no further change until end point (Figure 8). These alterations occur when the total percentage of myofibres IR to MyHC3 remains fairly constant while the number of hybrid fibres increase by ~50% (Figure 8).

The fraction of enclosed type-I myofibres, increased from 23%-to-50% from young adulthood to endpoint and in parallel with an increased prevalence of type-I myofibers (Figure 9, upper panel). The observations are scattered around the lines for the expected degree of enclosure based on type prevalence and number of fibre-neighbours; the difference between observed frequency and that expected by a random distribution was not significant (p=0.159, t-test pairs) across ages (Figure 9)
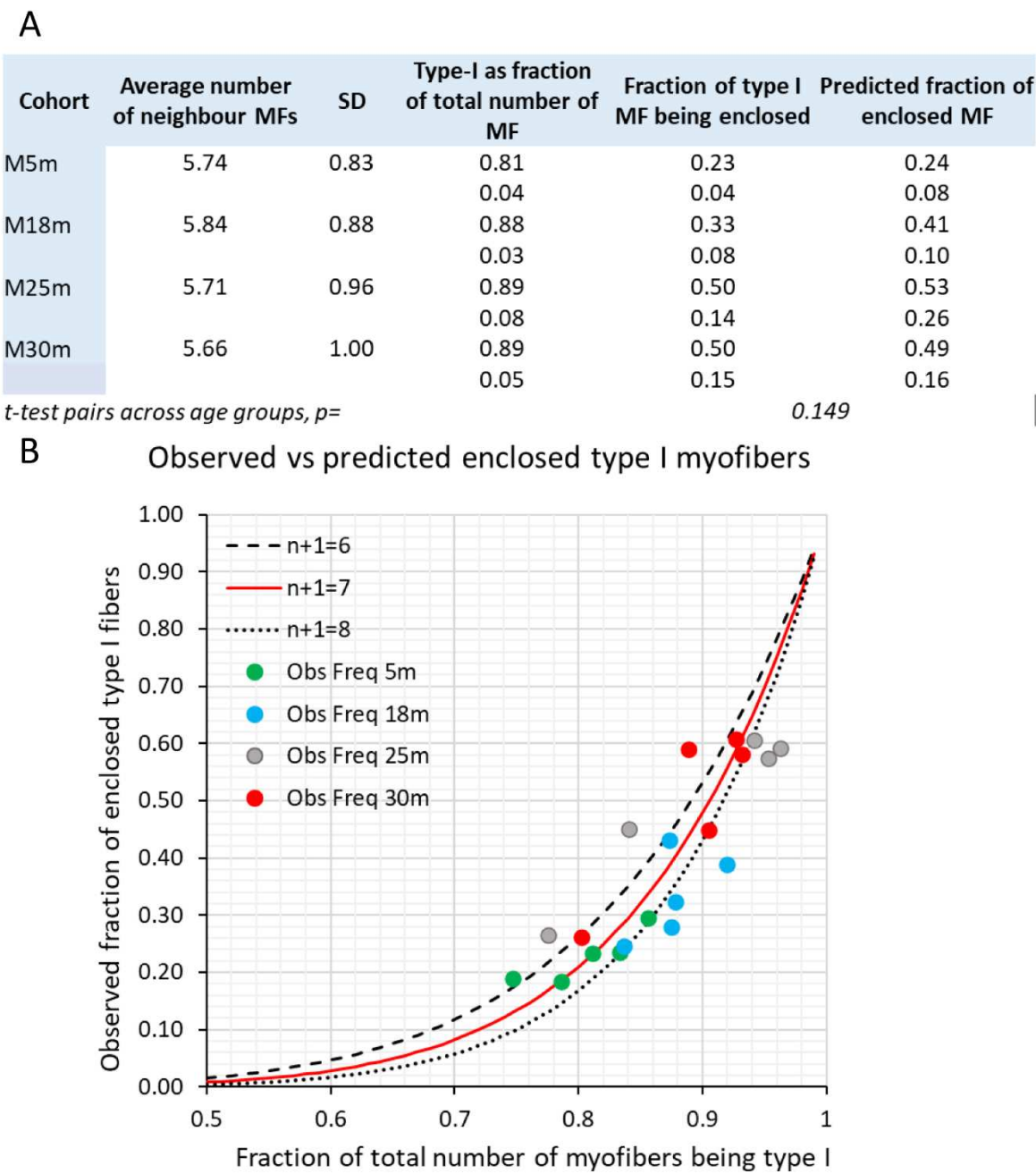
Importantly, these processes which result in a substantial loss of muscle mass, also in relation to the whole-body weight appear not to involve a change in the number of myofibers in m soleus (Supportive information (Figure S7)). Several of the variables analysed here showed strong covariations, correlating directly or inversely with each other, and with normalized soleus mass, gait score and age (Figure 10).
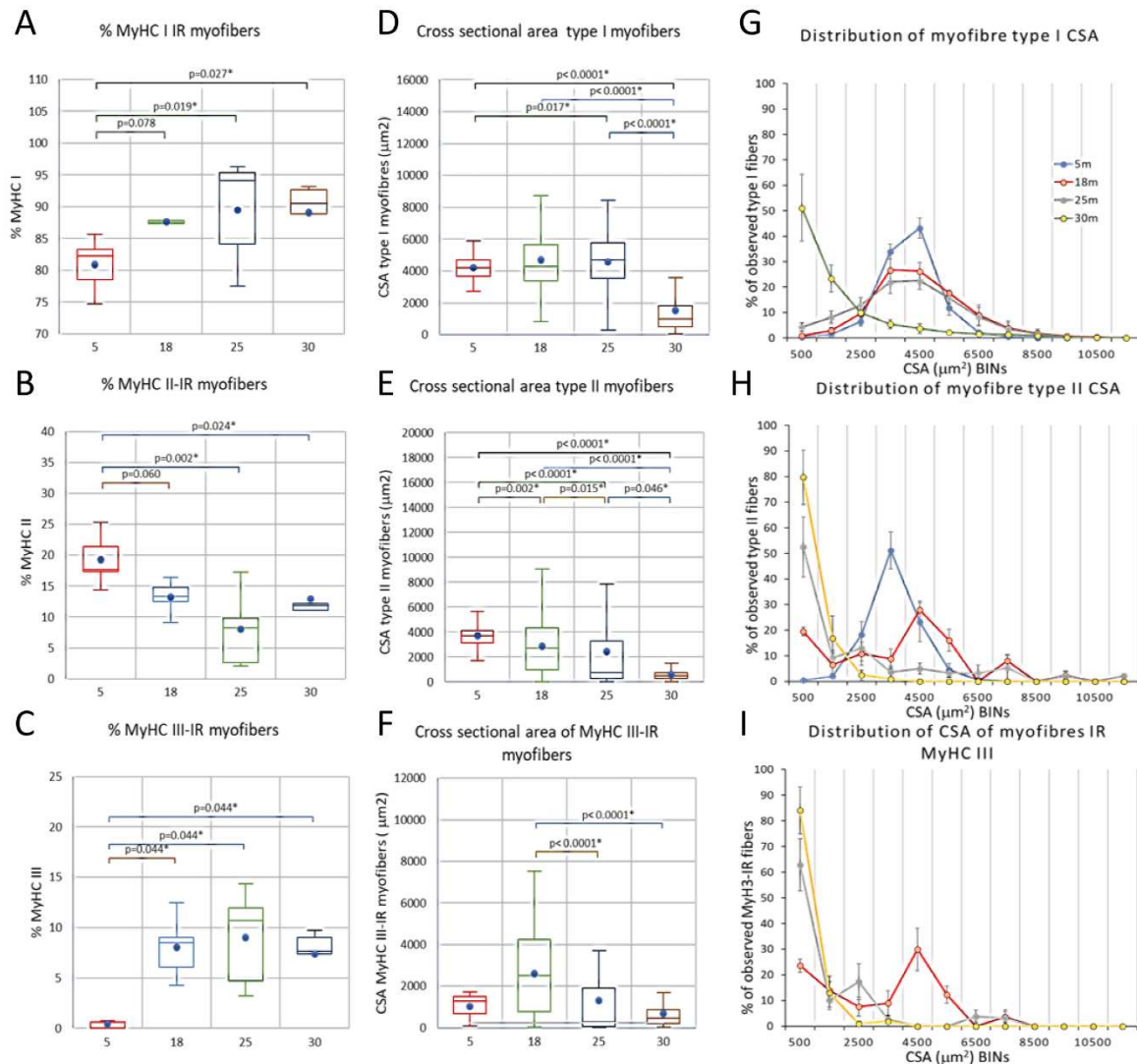


**Figure 7.** Boxplots of metrics (A-F) on m soleus during aging. Age groups have been indicated on the abscissa and metric on the ordinate in A-F. Kruskal-Wallis analysis of variance indicated that each metric changed in significantly during aging. Pair-wise post hoc testing results have been indicated where they were significant. G-I plots showing the distribution of CSAs (in BINs of 1000μm²) for type I (G), type II (H), and embryonic myosin (I) expressing myofibers.
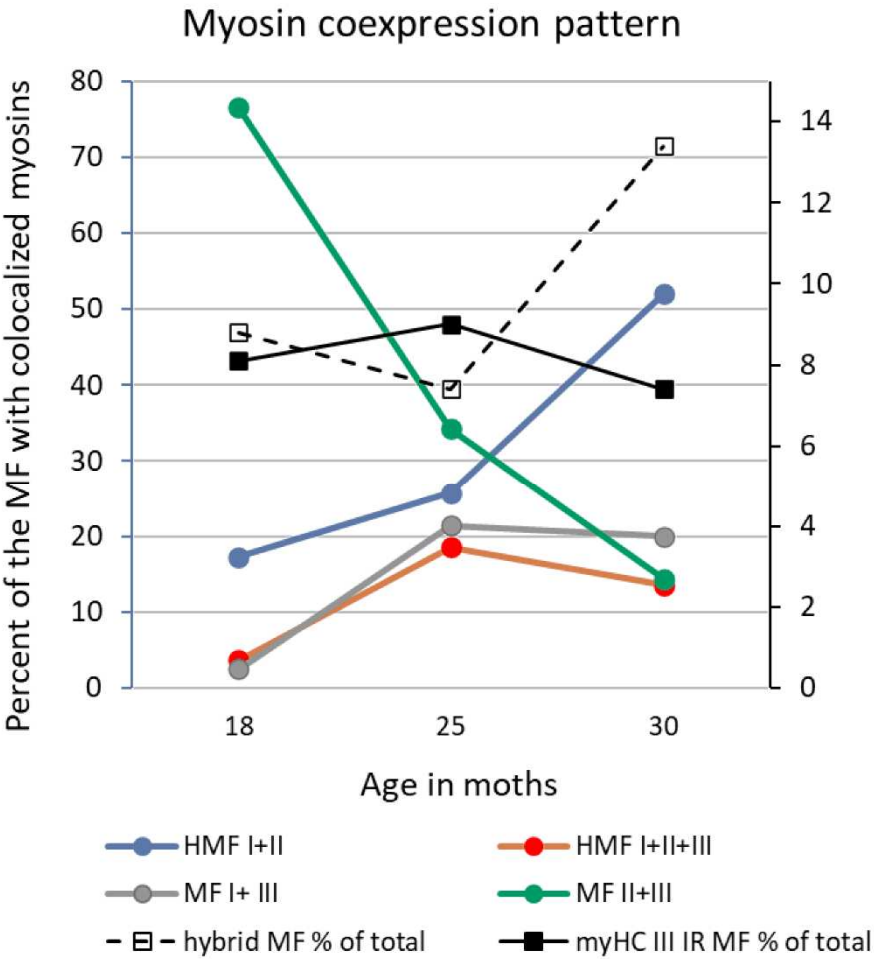
**Figure 8.** Plot showing the relative change between 18-25-30 month old rats (abscissa) in percent (left ordinate) of the myofibers (MF) expressing different combinations of myosins. The percentage of the total number of myofibres (ordinate to the right) in each age cohort expressing MyHC3 (black solid line) or being defined as a hybrid I/II fibre (HMF; interrupted black line). Data from young adult rats excluded because the prevalence of such fibres was <1%.

## A

| Cohort | Average number of neighbour MFs | SD | Type-I as fraction of total number of MF | Fraction of type I MF being enclosed | Predicted fraction of enclosed MF |
|---|---|---|---|---|---|
| M5m | 5.74 | 0.83 | 0.81 | 0.23 | 0.24 |
|  |  |  | 0.04 | 0.04 | 0.08 |
| M18m | 5.84 | 0.88 | 0.88 | 0.33 | 0.41 |
|  |  |  | 0.03 | 0.08 | 0.10 |
| M25m | 5.71 | 0.96 | 0.89 | 0.50 | 0.53 |
|  |  |  | 0.08 | 0.14 | 0.26 |
| M30m | 5.66 | 1.00 | 0.89 | 0.50 | 0.49 |
|  |  |  | 0.05 | 0.15 | 0.16 |

*t-test pairs across age groups, p=*      *0.149*

## B



**Figure 9.** A panel indicates mean and SD for number of myofiber neighbours, prevalence of type I myofibers, observed number of enclosed type I myofibres, and the predicted number of enclosed type I myofibers in each age cohort. B shows the observed fraction of enclosed type I myofibers (ordinate) plotted against the prevalence of type I myofibers. The three curves (solid, interrupted and dotted) show the expected number of enclosed myofibers by a random distribution as a function of type I prevalence (abscissa) if number of neighbours equal 6, 7 or 8, respectively (key in graph).

In summary, all muscle metrics except number of myofibers (KW p=0.295) showed significant changes across the adult lifespan (KW p<0.049 down to p<0.0001, Table 5; for pair-wise post hoc testing see the Supportive information (Figures S6 and S7)).
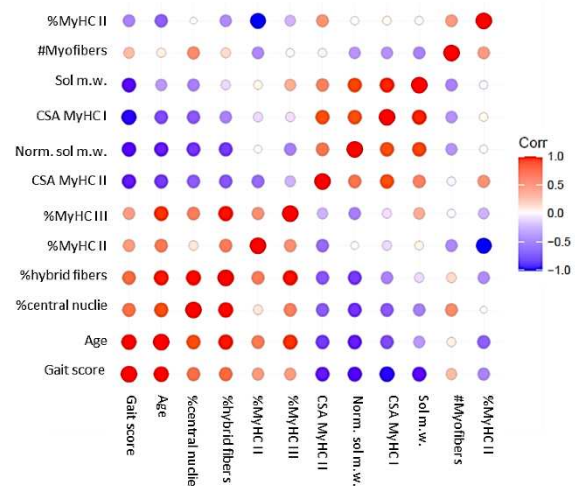
**Table 5.**

| Cohort | | Age | Central nuclei (%) | Pax7 IR profiles / myo-profile* | % Ki67-IR of Pax7-IR* |
|---|---|---|---|---|---|
| **M5m** | mean | 5 | 3.0 | 0.15 | 6.54 |
| **n=5** | ±SD | | 0.6 | 0.03 | 4.67 |
| **M18m** | mean | 18 | 8.1 | 0.24 | 3.08 |
| **n=5** | ±SD | | 3.2 | 0.09 | 4.21 |
| **M25m** | mean | 25 | 6.6 | 0.14 | 2.65 |
| **n=5** | ±SD | | 2.4 | 0.05 | 2.52 |
| **M30m** | mean | 30 | 16.0 | 0.05 | 3.94 |
| **n=5** | ±SD | | 7.6 | 0.02 | 4.28 |
| *KW* | *p=* | | *0.007* | *0.005* | *0.51* |
| *\* average # fibres ≥117 analysed* | | | | | |
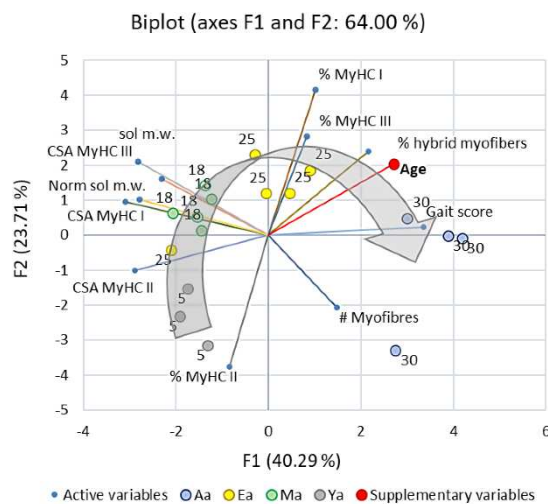


**Figure 10.** (A) PCA analysis of metrics on m. soleus in age-cohorts of male rats (5 (Ya), 18 (Ma), 25 (Ea) and 30 (Aa)-month-old) show covariance with 64% of the total variance explained by the two first principal components (F1 and F2). Note that age is a supplementary variable not contributing to the factor loading on the F1 and F2 axes. As the inserted arrow indicates, middle aged (Ma, 18) rats separate from young adult (Ya, 5) on F2 driven by the increase of hybrid and MyHC3-IR myofibers, and dropdown in number of type II fibres. As aging progresses the further separation is mainly along F1 (Ea 25 and Aa 30) driven by type II followed by type I myofiber atrophy, drop in soleus muscle weight, and emerging gait deficiencies. (B) Correlation coefficients between metrics in A have been colour coded with shades of red denoting positive correlations while shades of blue indicate an inverse correlation.

*Satellite cell number and co-immunoreactivity with Ki67*

Satellite cells (SC) were identified based on their anatomical location and for being Pax7 IR (Figure 11). SC number per fibre cross-sectional circumference showed a non-significant increase from 0.15 in young adults to 0.24 in 18-months-old rats followed by a gradual drop in density down to 0.05 SC per profile at endpoint (p<0.005, Table 6; for pairwise post hoc testing see Supportive information (Figure S8)). When SC density was included in the PCA, Pax7 correlated positively with Type I myofiber CSA (r=0.623), soleus muscle weight (r=0.70), normalized soleus mass (r=0.54) and inversely with gait score (r=-0.77) (all correlations p<0.05). The percentage of Pax7-IR nuclei also IR to Ki67 did not change significantly across adult lifespan (~4% of the Pax7-IR nuclei; Table 6).
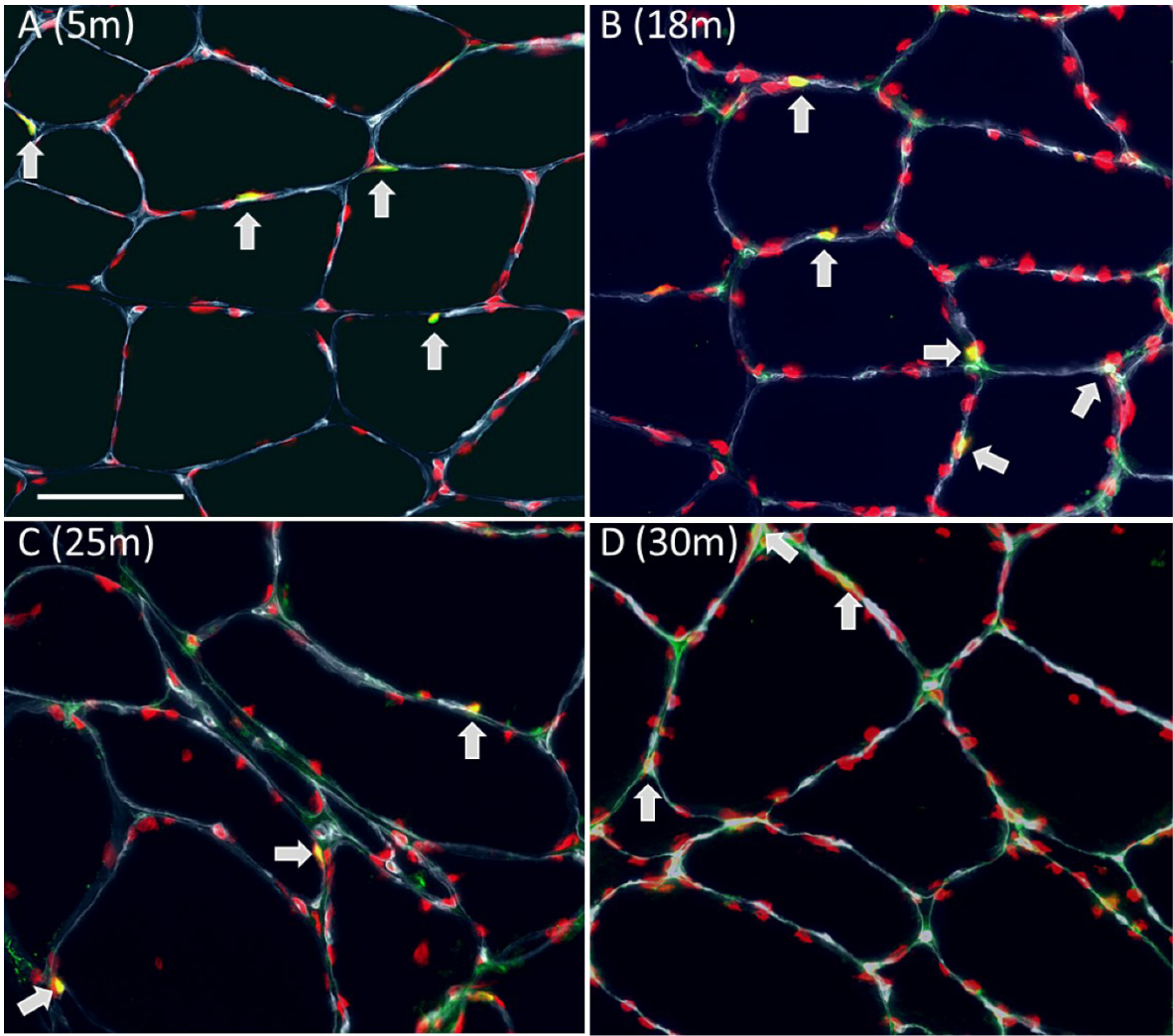
**Figure 11.** Pseudo-coloured three channel confocal images with DAPI (red), Pax7-IR (green) and laminin (blue) of samples from young adult (A), middle aged (B), early aging (C) and advanced age (D) rats. SC appear as yellow profiles (examples indicated by arrows) from the blending of red (DAPI) and green (Pax7-IR) light and are situated in the SC niche. Scale bar in A is 50 µm and applies to all panels.
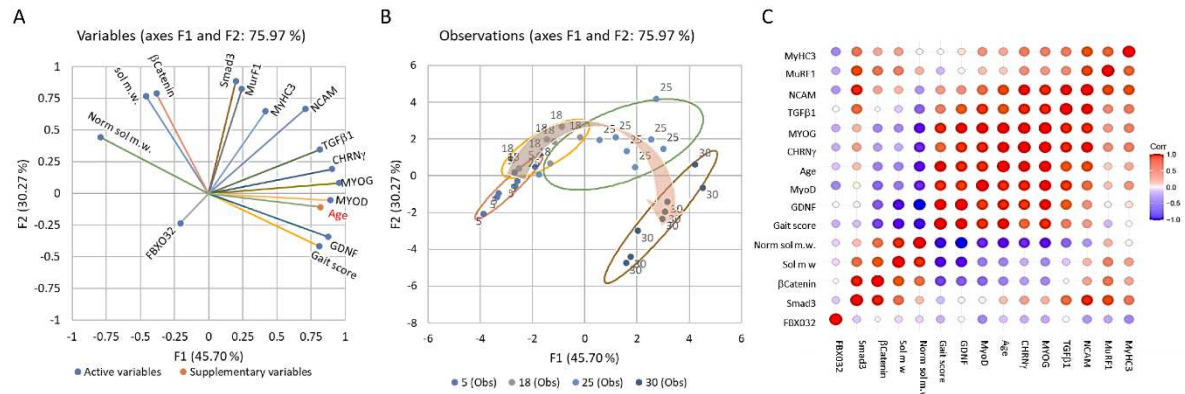
Table 5

*Analyses of skeletal muscle mRNA*

Male rats

Based on previous results a select panel of mRNA transcripts were analysed for abundance in male rat muscles (Material and methods; Figure 12).

**Figure 12.** (A) PCA analysis of gene expression across age groups of male SD rats reveal a high degree of direct or inverse covariance among the genes investigated with 76% of the total variance explained by the two first principal components. TGFβ1, CHRNγ, MYOG, MYOD and GDNF mRNAs formed one cluster of co-varying transcripts loading mainly on F1, while βCatenin, Smad3, MuRF1, and MyHC3 mRNAs formed another cluster loading mainly on F2. NCAM and FXBXO32 transcript levels loaded equally on F1 and F2. In (B) the observations in each age group have been indicated and the ovals stand for the 70% confidence limit of respective group. Compared with young adults, middle aged rats and rats in early aging separate gradually on both F2 and F1. The shift on F2 is driven by increased levels of βCatenin, Smad3, FBXO32, and MuRF1 transcripts. At advanced age (30) these transcripts become downregulated. Across the middle age, early and late aging there is a gradual increase in abundance of the transcripts loading on F1. Note that *Age* is a supplementary variable and does not contribute to the loading of F1 or F2. (C) Correlation coefficients between metrics in A have been colour coded with shades of red denoting positive correlations while shades of blue indicate an inverse correlation.

In male rats, all the mRNA transcripts analysed showed significant alterations in abundance during adult lifespan (KW p<0.042 down to p<0.0001). However, as shown in Figures 13–15, the regulation of several transcripts is complex and appears to mark successive events in the loss of muscle mass and function during aging.

Normalized soleus mass correlated inversely with abundance of GDNF (r=-0.88), MYOG (r=-0.69), MYOD (r=-0.65) and CHRNγ (-0.64) transcripts across age groups (all p<0.05). Gait score showed an equally strong covariation with these transcripts (GDNF, r=0.85; MYOG, r=0.74; MYOD, r=0.73; CHRNγ, r=0.58) (Figures 12, 13 and 15). A similar pattern was also evident for TGFβ1 mRNA expression (Figures 12 and 14). In contrast, the intercorrelated transcript levels of βCatenin, Smad3 and MuRF1 showed an initial increase followed by a downregulation at end point (Figure 14).
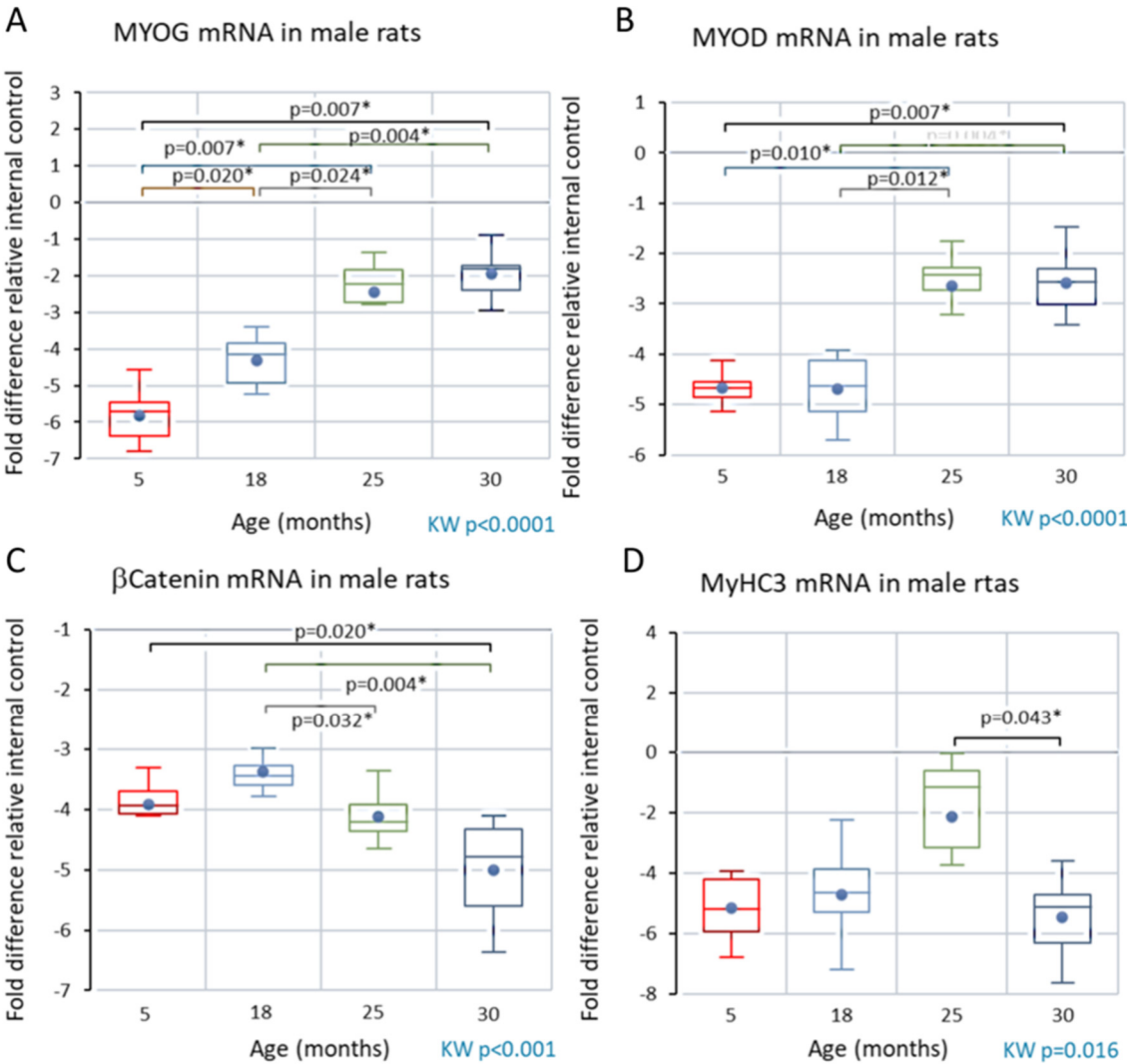
**Figure 13.** Boxplots of MYOG, MYOD, βCatenin, and MyHC3 mRNA expression m soleus during adult lifespan in male rats. Age groups have been indicated on the abscissa and fold difference relative internal control on the ordinate. Kruskal-Wallis analysis of variance indicated that each mRNA changed in significantly during aging (see KW in panels). Pairwise post hoc testing results have been indicated when significant.
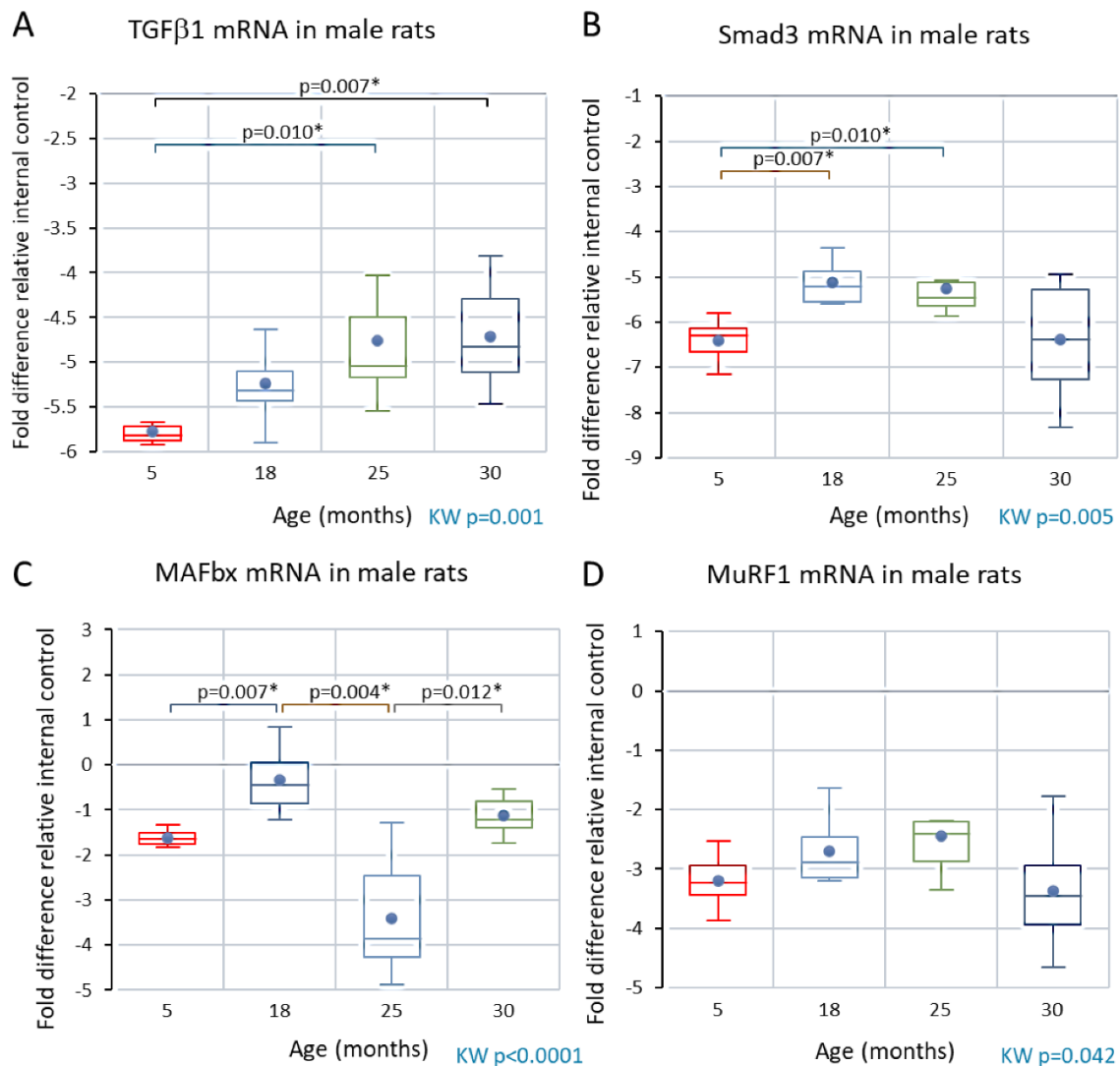
**Figure 14.** *A-D* Boxplots of TGFβ1, Smad3, FBXO32 and MurF1 mRNA abundances in m soleus during adult lifespan in male rats. Age groups have been indicated on the abscissa and fold difference relative internal control on the ordinate. Kruskal-Wallis analysis of variance indicated that each mRNA changed in a significantly during aging (see KW in panels). Pairwise post hoc testing results have been indicated where they were significant.

Comparison of CHRNγ, MYOG, NCAM and GDNF mRNAs in aging male and female rats, and in the response to axotomy.

The variation in expression of CHRNγ, GDNF, NCAM and MYOG mRNAs was assessed in young adult, middle aged and endpoint female rats and showed the same pattern of regulations as those described above for male rats (Figure 15, see Supportive information (Figure S9)). In addition, CHRNγ, GDNF, NCAM mRNA abundance was also assessed in young adult females rats 10 days following a complete sciatic axotomy. As shown in Figure 15 (G-I), the regulation of these transcripts in response to axotomy are like those occurring during normal aging.
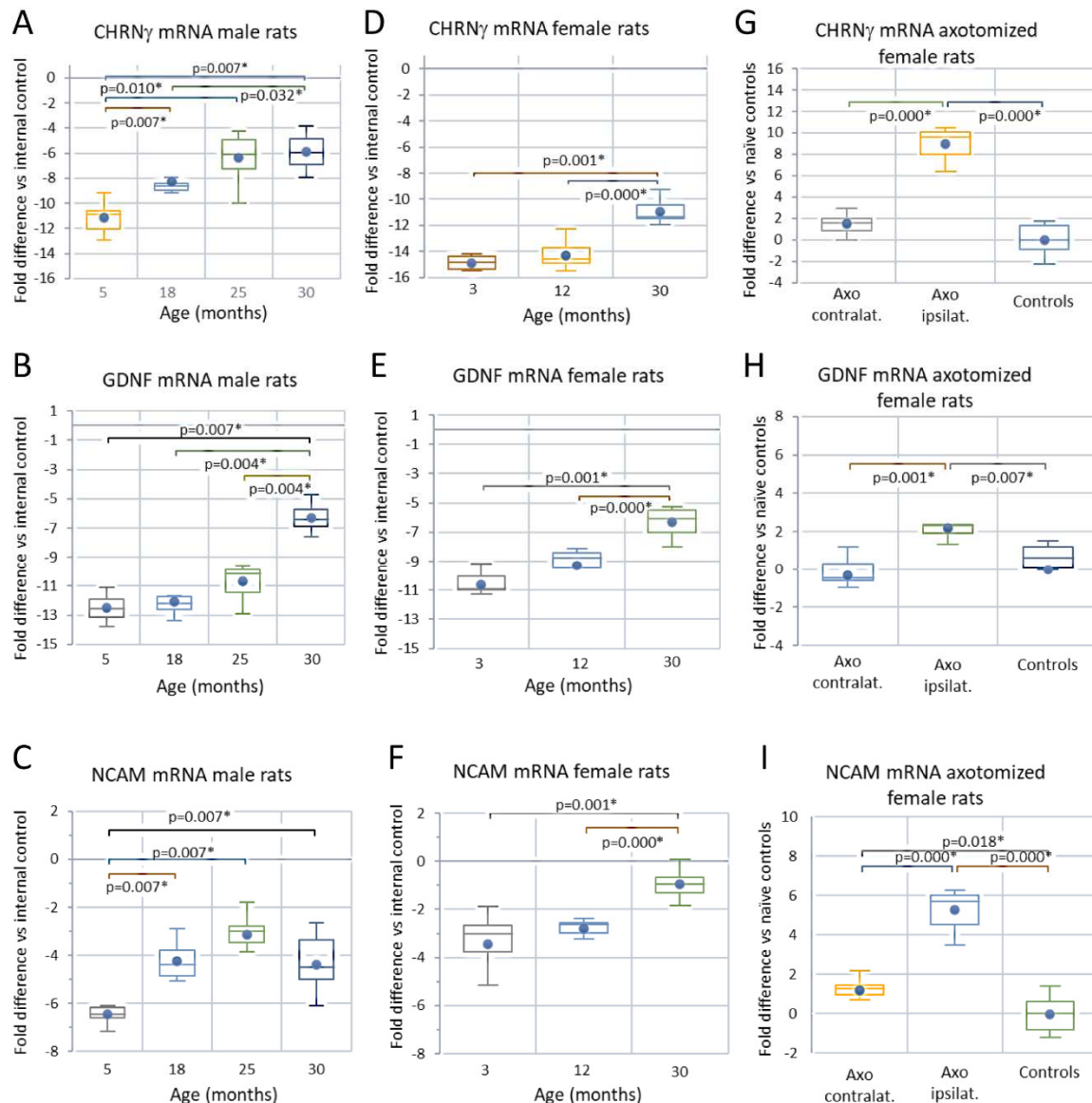
**Figure 15.** Boxplots of CHRNγ GDNF, NCAM mRNA abundance in m soleus during aging in male (A, B, and C), and female (D, E, and F) rats. In panels G, H, and I) the muscle response ten days after a complete unilateral axotomy in a young adult female rat. Age groups have been indicated on the abscissa and fold difference in mRNA level relative internal control on the ordinate in A-F. In panels G-I the transcript level on the ipsilateral and contralateral side is shown along with naïve controls (used for normalization). Kruskal-Wallis analysis of variance indicated that each metric changed in a significant way during aging and in response to axotomy. Pairwise post hoc testing results have been indicated where they were significant.

## Discussion

*General comments and limitations of this study*

Small rodents are used as models on sarcopenia since these species mimics the clinical phase of the human condition[15,31,62,75–77] and we chose rats, rather than mice, because available data suggests that the sarcopenia process in rats is more similar to the human counterpart (*idem*). We selected an outbred rat strain to capture the variability in emergence and progression of sarcopenia, and the results show that endpoint rats doing-well had outcomes like an average early-aged-rat and vice versa. Thus, the variance between chronological and biological age seen here in the rat resembles the situation reported in humans. Sarcopenia in humans is brought to our attention once the

condition infringes on physical activity of every-day-life or e.g., results in a fall related fracture. Thus, in this study we used motor capacity and coordination indices along with relative muscle mass as key metrics of sarcopenia. We placed the emphasis on gait performance because this entity appears to be a good biomarker for human sarcopenia (see Introduction) and translates well between species[64,75,78].

We used the soleus component of hind limb triceps surae muscle. The rationales for selecting this muscle were its frequent use and long duty cycle in every-day motor behaviours of the freely moving rat[63], and an ankle extensor muscle is highly relevant since rats normally stride on their toes. The drawback is that morphological and transcriptional data on humans usually derive from the vastus lateralis component of musculus quadriceps femoris (an extensor of the knee joint) mainly because it is readily accessible for tissue sampling.

In this study no net change in the number of myofibers of the soleus muscle across adult life span could be detected. Our data on fibre numbers agrees with earlier observations made in this species ([73,79] and was assessed in a complete cross-section at a distance from its origin where most if not all fibres should be present. While loss of myofibers have been reported in the m. vastus lateralis in humans, it is also known that the sarcopenia process impacts muscles differentially and m. soleus serving as an anti-gravity postural muscle with long duty cycles is affected at a later stage and to a lesser extent than for example the components of m. quadriceps (for review see [80]). Incapacitation of m soleus marks a progression stage of sarcopenia where individuals are unable to maintain an independent lifestyle. This was also the case for many subjects in the endpoint group of this study being unable to reach the food hooper or nipple of the water bottle (see Material and methods).

We used embryonic myosin (MyHC3), NCAM and CHNR-γ in parallel as markers of myofiber denervation. MyHC3 is normally supressed in adult muscle but re-expressed following denervation and re-suppressed upon re-innervation (in the rat, [66]; reviewed in [81]) and often used as marker for denervation in studies of aging ([64]). NCAM (neuronal cell adhesion molecule) mRNA is also frequently used marker for denervation ([82]; reviewed in [83]). Sanes and colleagues showed that NCAM protein associates with the postsynaptic membrane of the NMJ ([84]) and, moreover, that disturbance of the NMJ integrity results in an upregulation of NCAM by the myofiber (idem). However, using either one of NCAM and ;yHC3 as denervation marker may underestimate the true number because these proteins are not distributed uniformly along the length of a myofibre ([82]). As a third marker for denervation, we assessed the mRNA expression of CHNR-γ subunit. The CHNR is composed of five subunits which changes in composition from                to                during development but reverts back in response to denervation ([66,85]). In adult rats, the re-expression is re-supressed following successful re-innervation ([66]). As recently shown, reversible changes of the expression of the markers neonatal MyHC (MyHC8), NCAM and CHNR-γ can also be induced by muscle unloading alone ([86,87]), an intervention that in addition induce changes to the prevalence of fast and slow myofibers and their degree of fibre-type grouping (*idem*, see above).Thus, the currently deployed markers for myofiber denervation cannot safely make a distinction between changes induced by nerve damage and unloading. Another marker used for myofiber denervation not included here, is the relative expression of the voltage-gated sodium channels Nav1.4 and Nav1.5 [88,89]. However, as shown elsewhere, Nav 1.4 and Nav1.5 are differently regulated depending on context ([90,91]) and neither Nav1.5 nor NCAM is consistently induced by denervation in young and old rats ([83]).

The mRNA transcript analyses were conducted on whole muscle samples and can thus not provide information about which cell type(s) expressed the different mRNAs. The selection of transcripts analysed herein was based on results in our previous longitudinal study of muscle aging in humans[92] and the temporal pattern of transcript regulations in the response to peripheral nerve crush in female rats[66].

A further limitation of this study is the cross-sectional design (for discussion on study design and references see[92] ). However, we believe this is less of a problem with rats since lifespan is comparatively short and living conditions can be kept highly reproducible across age groups.

*Natural history of sarcopenia in the rat*

Preclinical phase of sarcopenia

The results show that motor performances as gait and coordination remain intact through the middle age (12-18 months) when muscle mass relative to body weight is largely maintained. The muscle, however, shows multiple signs of remodeling [adaptations] with a shift in myofiber-type composition towards type I, increased number of hybrid fibers and of, in particular, type II fibers expressing embryonic myosin. A pattern-shift apposite that observed following soleus muscle unloading or nerve damage in young adult rats ([66,93] ). In late middle age almost 10% of mainly type II myofibers co-express MyHC3 and in parallel the number hybrid fibres raise to the same level. However, these two fibre subpopulations are not completely overlapping, implicating that some hybrid fibres have been re-innervated and do not express embryonic myosin. Also considering the parallel decrease in number of type II fibres between adulthood (19%) and late-middle age (13%), the pattern-shift in late middle age is not likely induced by sustained unloading or timed nerve damage but as suggested Lexell and coworkers [22] by repeated cycles of denervation [of preferentially type II myofibers] followed by collateral re-innervation [by motoneurons innervating type I myofibers]. The increase of MyHC3-IR protein and mRNA correlated with a robust upregulation of NCAM (neuronal cell adhesion molecule), nicotinic acetylcholine receptor subunit γ (CHRNγ ), and MYOG mRNA. The covariation of NCAM, MYOG and CHNR-  mRNA upregulations observed here in aging male and female rats is similar to that occurring in response to experimental denervation in young adult rats (this study and [11]) and in-line with corresponding data from aging female but not male humans [18,19].

The latter combined with a transcriptional upregulation of and NCAM suggests that the remodeling is driven by a process of fiber denervation of type II myofibers belonging to fast twitch MUs, followed by a collateral re-innervation from intact axons innervating nearby type I myofibers of slow twitch MUs. That recruitment order and firing rate of the innervating motoneurons impact the contractile properties of the target myofibers are well known since the classical cross-innervation experiments half a century ago[94]. The selective vulnerability of myofibers in fast twitch MU has not been clarified. However, as suggested elsewhere the vulnerability may stem from their much more extensive axonal arborization and   larger number of axons terminals which may create a greater metabolic burden than must be carried by motoneurons of the smaller-sized slow-twitch MUs[8].

Repeated cycles of denervation-reinnervation may cause a shift in fiber type prevalence and a clustering of fibers with similar expression of contractile proteins (fiber type grouping) and expand the size of slow twitch MU [57,75–77]. Jennekens and colleagues brought our attention to that the mosaic pattern of myofiber type distribution within a mixed muscle differed among human skeletal muscles and, moreover, is impacted by myo-pathological processes including aging[35,67]. The increased fibre-type grouping observed during aging were later confirmed and extended by Lexell and coworkers [95,96]. We observed an increase from ~20% up to ~50% of enclosed type I myofibers in the soleus muscle during aging (see also [54]). In our material, the observed number of neighbours of a type I fibre came very close to the assumed model of a hexagonal lattice array arrangement of cross-sectioned myofiber profiles in all age groups, and with a standard deviation of close to 1. Furthermore, ~70% of our observations on the frequency of enclosed type-I fibres were within ±1 SD ($p^6$ to $p^8$) of that expected from the prevalence of type-I fibres in the different age groups. The results obtained here agrees with those recently reported for sedentary and exercised aging humans[97] and suggest that the degree, or changes in the degree, of fibre type grouping may be driven by an underlying shift in the prevalence of a myofiber type (see also [98,99]). However, there is also data from human vastus lateralis muscle, showing an increased type I clustering in the absence of any change to fibre type prevalence [100].

In the preclinical phase of sarcopenia when the rats were behaviorally asymptomatic, we recorded a small drop in normalized soleus mass, and a significant reduction in CSA (-15%) among the remaining type II myofibers. The concurrent decrease in the number and CSA of type II myofibers and the increase in the number (+8%) and small increase in CSA (+9%) of type I myofibres appear to largely balance resulting in a fairly stable relative muscle mass. It is notable that in contrast to more

advanced ages, myofibers expressing MyHC3 in the late middle age are not severely atrophied. This may be interpreted as re-innervation at this stage is fairly rapid and frequently successful. This may help to explain the absence of behavioral signs in e.g., gait.

In the preclinical phase during late middle age, we recorded a doubling in number of nuclei with a central position of the myofibers and a robust upregulation of MYOG transcripts (member of the myogenic differentiation factor (MDF) family).   In parallel there was a slight (statistically not significant) increase of Pax7 IR nuclei in the satellite cell (SC) niche and increase of βCatenin mRNA. These changes suggest that the SC population density and some of the proteins involved in SC replication and subsequent differentiation to myocytes (MYOG and MYOD) are at least maintained at the level of young adult rats. The early upregulation of MYOG may also relate to MDFs being implicated in stabilizing the NMJ [121].

In experimental or disease related atrophy of skeletal muscle, activation of FOXO transcription factors by an increased Smad signaling (e.g., downstream of Myostatin activation of the Activin receptor 2) induce regulated proteolysis targeting contractile muscle proteins through activation of the ubiquitin-proteasomal system (UPS) including the muscle enriched E3 ligases FBXO32 (MAFbx, atrogin) and MuRF1 [101–106]. Our results show that Smad3, FBXO32 and MuRF1 (the latter not statistically significant) transcripts increase in skeletal muscle during late middle age accompanying the adaptive changes of the late middle-age. We recently reported in a longitudinal study of a human cohort (ULSAM, males subjects), that the vastus lateralis muscle of m. quadriceps showed increased levels of Smad2 and MurF1 mRNAs in early aging (70 years old) while these upregulations were attenuated when the subjects were re-examined at age 88 years of age[71]. The activation of the UPS during the preclinical phase of sarcopenia may be a prerequisite for the remodeling needed to adapt to the ongoing denervation-reinnervation process[71,107]. At early aging, these ULSAM subjects also showed upregulations of MYOG, MYOD, NCAM and MyHC3 mRNAs (*idem*), very similar to the regulatory pattern found here in late middle-age and early aging rats.

Clinical phase of sarcopenia

Much more is known about the clinical than the preclinical phase of sarcopenia and the results obtained in this study are at large in agreement with previous studies on male and female rats, and humans. Briefly, in early (25-month-old) and late (endpoint, 30-month-old) aging, motor performance as gait and limb coordination deteriorate as muscle mass is lost (in relative terms >50% at endpoint). This is a gradual transition varying in pace and extent between subjects, e.g., some 25-month-old rats were still functionally intact while others displayed serious behavioral deficits. In relation to expected median lifespan, the 25-month-old cohort corresponds to humans at the age of 60- to 70-years old. At the level of the muscle, there is a reduction in both absolute and relative soleus muscle mass, frequency, and CSA of type II fibers, while type I fiber CSA is still maintained at young adult level. The occurrence of hybrid- and MyHC3-IR myofibers remain about the same as in the late middle age. A marked difference compared to rats in the late middle age, is the significant atrophy of MyHC II- , hybrid- and MyHC3-IR myofibers along with a further upregulation of CHRNγ, NCAM and MYOG mRNAs. This may be interpreted as denervated myofibers to some extent remain denervated at least for a longer while allowing time for an accentuated myofiber atrophy and tissue accumulation of mRNA-markers of disturbed innervation. Another important difference is that in early (and late) aging an increasing number of type I myofibers express embryonic myosin indicating that this subpopulation of MUs becomes affected to a larger extent. Combined these changes might explain why clinical symptoms emerge at this stage while relative muscle mass is still reduced by only ~20%. Progressive failure of collateral re-innervation with advancing age has also been proposed to occur in humans[55,57] when sarcopenia becomes clinically overt[21,57,108–112]. In early aging, the density of Pax7-IR nuclei and level βCatenin mRNA was lower than in 18-month-old but still en-par with our observations in young adult rats, and the marker we used as indicator of SC replication rate in vivo (Ki-67 IR;[68,113]) did not indicate a significant change across adult lifespan (see also below). In early aging we observed a transcriptional co-upregulations of TGFβ1 and MYOD (member of the MDF family) mRNAs not present in the middle ages, a co-regulation of these two transcripts appear to

play a role in the myogenic differentiation process [114,115] suggesting that more SC offspring differentiate into myocytes than in late middle life. However, both MYOD and MYOG have also been associated with other remodelling processes such as the myofiber response to denervation [107,116–119].

As aging progresses towards the endpoint, myofiber atrophy accelerates and also involves MyHC I-IR fibers (>50% reduction in CSA; see also [120]). Muscle mass is lost at high pace also in relative terms (- 60%) and motor performance and coordination deteriorate. We confirm previous observations that mRNA transcripts associated with increased proteolysis of contractile proteins and MyHC3 return towards base-line values at advanced age[69,70,92,121], while the MDFs and CHRNγ transcripts remain elevated and the percentage of myofibers with nuclei in a central position continues to increase. Also in these respects, the current results in aging rats are in line with longitudinal observations made on aging males in the ULSAM cohort[71].   Our observations in rats at advanced age, suggests that remodeling and regeneration fades but does not cease. At this stage, there is a significant depletion of Pax7-IR nuclei in the SC niche while the replication rate among remaining SC was unchanged compared to late middle age and early aging. A depletion of SC at advanced age confirms previous studies on small rodents and humans alike, while the maintained replication rate is at variance with earlier observations [44,45,122,123]. There are two not mutually exclusive explanations to this discrepancy. First, previous studies on replication rate were done on harvested SC *ex vivo* and may not reproduce replication rate *in vivo* considering the multitude of changes occurring in the muscle scaffold and SC niche during advanced aging. We used Ki67-IR as a proxy for SC replication and albeit its wide use in grading tumors aggressiveness by cell division propensity[68,113] it has not been validated for SCs in an aged SC niche. Furthermore, colocalization of Pax7 and Ki67 IR proteins does not implicate by necessity that SC offspring's commits to, and successfully pursue a maturation into myocytes. Furthermore, we have examined rather few subjects in each age group. Thus, this issue deserves further attention.

At advanced age we noted a marked increase of glial-derived nerve growth factor (GDNF) mRNA which confirms our previous observations[124,125] and is in-line with data from humans[126]. GDNF is a target derived neurotrophic factor retrogradely transported to motoneurons and critical for perinatal survival for a subpopulation of spinal motoneurons [127,128] while the function of GDNF at later stages is not fully understood. In adulthood, GDNF may be important for NMJ maintenance and re-innervation since it is promptly upregulated in response to axon damage [126]. GDNF interacts also with the GRF-1   receptor and NCAM in the myofiber, and NCAM has been proposed as an interaction partner in the collateral re-innervation processes[109,129]. However, our data on rats show that NCAM upregulation precedes that of GDNF. Thus, these changes appear not be temporarily coordinated on the transcriptional level during aging. The significance of very high levels of GDNF transcripts at the endpoint remains unclear and needs further study.

At more advanced stages of aging there are highly significant changes to the cellular composition of the skeletal muscle, with inter- and intra-myofiber infiltration of fat and a low-level inflammation possibly driven by intramuscular degenerative processes, and an accumulation of senescent cells and the impact of their secretome ([33,58,59]). In parallel, there is a significant accumulation of extracellular matrix and changes to the matrix components [130–132] and a multitude of changes to the muscle transcriptome and proteome [60]. Already one-by-one and, in particular, when occurring concurrently these changes will transform the muscle scaffold to an environment that is unlikely to facilitate and promote adaptations and regeneration of myofibers in generic MUs of the muscle [132,133]. It is therefore very encouraging that physical exercise can improve motor behaviour also in very old people when muscle mass does not increase in response to exercise [134–136].

**Concluding remarks**

Our data support previous observations that gait (stride) is a sensitive biomarker of sarcopenia [and aging][15,31,65,75,78,137] correlating closely with relative muscle mass in rats. The muscle wasting during aging is initially owing to type II myofiber atrophy driven by fiber denervation

followed by a collateral re-innervation creating a shift with increased type I dominance and a growing population of hybrid and MyHC3 expressing myofibers. This latter process made up for most of the type II atrophy in late middle age so relative muscle mass decrease was limited to ~10% and the subjects remained behaviorally intact (preclinical phase). During early aging, myofiber atrophy progresses affecting both type II and MyHC3 expressing myofibers, suggesting delayed or even failed re-innervation. Although relative muscle mass loss still was modest (~-20%), gait and coordination were impacted (clinical phase). In the further progression into advance age (endpoint), relative muscle mass loss is massive (relative mass down by ~50% from early aging to endpoint) involving all myofiber types and, in parallel motor performance deteriorates to the degree that several rats could not even manage motor activity of everyday life (food and drink had to be served at the level of the cage floor). Our data suggests that rats can serve as a useful model of preclinical sarcopenia in humans. Interventions supporting the intrinsic adaptive mechanism in operation at this age and impeding further progression into clinical sarcopenia may prove more rewarding than addressing this clinical condition once it has become clinically manifest. Gait (and similar motor dependent behaviors), relative muscle mass, expression of embryonic myosin, and the expression level of NCAM and CHRNγ appear to be useful biomarkers of sarcopenia progression in rats and humans alike.

## References

1. A LIFECOURSE APPROACH TO HEALTH. WHO/NMH/HPS/00.2
2. A.J. Cruz-Jentoft, J.P. Baeyens, J.M. Bauer, Y. Boirie, T. Cederholm, F. Landi, F.C. Martin, J.P. Michel, Y. Rolland, S.M. Schneider, E. Topinkova, M. Vandewoude, and M. Zamboni, Sarcopenia: European consensus on definition and diagnosis: Report of the European Working Group on Sarcopenia in Older People. Age Ageing 39 (2010) 412-23.
3. A.J. Cruz-Jentoft, G. Bahat, J. Bauer, Y. Boirie, O. Bruyère, T. Cederholm, C. Cooper, F. Landi, Y. Rolland, A.A. Sayer, S.M. Schneider, C.C. Sieber, E. Topinkova, M. Vandewoude, M. Visser, and M. Zamboni, Sarcopenia: revised European consensus on definition and diagnosis. Age Ageing 48 (2019) 16-31.
4. L.K. Chen, J. Woo, P. Assantachai, T.W. Auyeung, M.Y. Chou, K. Iijima, H.C. Jang, L. Kang, M. Kim, S. Kim, T. Kojima, M. Kuzuya, J.S.W. Lee, S.Y. Lee, W.J. Lee, Y. Lee, C.K. Liang, J.Y. Lim, W.S. Lim, L.N. Peng, K. Sugimoto, T. Tanaka, C.W. Won, M. Yamada, T. Zhang, M. Akishita, and H. Arai, Asian Working Group for Sarcopenia: 2019 Consensus Update on Sarcopenia Diagnosis and Treatment. J Am Med Dir Assoc 21 (2020) 300-307.e2.

5. S.A. Studenski, K.W. Peters, D.E. Alley, P.M. Cawthon, R.R. McLean, T.B. Harris, L. Ferrucci, J.M. Guralnik, M.S. Fragala, A.M. Kenny, D.P. Kiel, S.B. Kritchevsky, M.D. Shardell, T.-T.L. Dam, and M.T. Vassileva, The FNIH Sarcopenia Project: Rationale, Study Description, Conference Recommendations, and Final Estimates. The Journals of Gerontology: Series A 69 (2014) 547-558.

6. L. Cao, and J.E. Morley, Sarcopenia Is Recognized as an Independent Condition by an International Classification of Disease, Tenth Revision, Clinical Modification (ICD-10-CM) Code. J Am Med Dir Assoc 17 (2016) 675-7.

7. T.A. Churchward-Venne, M. Tieland, L.B. Verdijk, M. Leenders, M.L. Dirks, L.C. de Groot, and L.J. van Loon, There Are No Nonresponders to Resistance-Type Exercise Training in Older Men and Women. J Am Med Dir Assoc 16 (2015) 400-11.

8. T. Gustafsson, and B. Ulfhake, Sarcopenia: What Is the Origin of This Aging-Induced Disorder? Frontiers in Genetics 12 (2021).

9. S. Phu, D. Boersma, and G. Duque, Exercise and Sarcopenia. J Clin Densitom 18 (2015) 488-92.

10. J. McKendry, L. Breen, B.J. Shad, and C.A. Greig, Muscle morphology and performance in master athletes: A systematic review and meta-analyses. Ageing Res Rev 45 (2018) 62-82.

11. D.T. Kirkendall, and W.E. Garrett, Jr., The effects of aging and training on skeletal muscle. Am J Sports Med 26 (1998) 598-602.

12. S. Trappe, Master athletes. Int J Sport Nutr Exerc Metab 11 Suppl (2001) S196-207.

13. B. Ganse, A. Kleerekoper, M. Knobe, F. Hildebrand, and H. Degens, Longitudinal trends in master track and field performance throughout the aging process: 83,209 results from Sweden in 16 athletics disciplines. Geroscience 42 (2020) 1609-1620.

14. E. Edstrom, M. Altun, E. Bergman, H. Johnson, S. Kullberg, V. Ramirez-Leon, and B. Ulfhake, Factors contributing to neuromuscular impairment and sarcopenia during aging. Physiol Behav 92 (2007) 129-35.

15. S.B. Ballak, H. Degens, A. de Haan, and R.T. Jaspers, Aging related changes in determinants of muscle force generating capacity: a comparison of muscle aging in men and male rodents. Ageing Res Rev 14 (2014) 43-55.

16. R.T. Hepple, and C.L. Rice, Innervation and neuromuscular control in ageing skeletal muscle. J Physiol 594 (2016) 1965-78.

17. L. Larsson, H. Degens, M. Li, L. Salviati, Y.I. Lee, W. Thompson, J.L. Kirkland, and M. Sandri, Sarcopenia: Aging-Related Loss of Muscle Mass and Function. Physiol Rev 99 (2019) 427-511.

18. E. Gutmann, Age changes in the neuromuscular system [by] E. Gutmann and V. Hanzlikova, Scientechnica, Bristol, 1972.

19. M. Brown, and E.M. Hasser, Complexity of age-related change in skeletal muscle. J Gerontol A Biol Sci Med Sci 51 (1996) B117-23.

20. M.R. Caccia, J.B. Harris, and M.A. Johnson, Morphology and physiology of skeletal muscle in aging rodents. Musc. Nerve 2 (1979) 202-212.

21. J.L. Rosenheimer, and D.O. Smith, Differential changes in the end-plate architecture of functionally diverse muscles during aging. J Neurophysiol 53 (1985) 1567-81.

22. K. Fujisawa, Some observations on the skeletal musculature of aged rats. I. Histological aspects. J Neurol Sci 22 (1974) 353-66.

23. K. Fujisawa, Some observations on the skeletal musculature of aged rats. Part 2. Fine morphology of diseased muscle fibres. J. Neurol. Sci. 24 (1975) 447-469.

24. E. Gutmann, and V. HanzlÍKovÁ, Motor Unit in Old Age. Nature 209 (1966) 921-922.

25. E. Gutmann, V. Hanzlíková, and F. Vyskočil, Age changes in cross striated muscle of the rat. The Journal of Physiology 216 (1971) 331-343.

26. T. Ansved, and L. Larsson, Quantitative and qualitative morphological properties of the soleus motor nerve and the L5 ventral root in young and old rats. J. Neurol. Sci. 96 (1990) 269-282.

27. L. Larsson, Motor units: remodeling in aged animals. J Gerontol A Biol Sci Med Sci 50 Spec No (1995) 91-5.

28. L. Larsson, Morphological and functional characteristics of the ageing skeletal muscle in man. A cross-sectional study. Acta Physiol Scand Suppl 457 (1978) 1-36.

29. E. Edstrom, and B. Ulfhake, Sarcopenia is not due to lack of regenerative drive in senescent skeletal muscle. Aging Cell 4 (2005) 65-77.

30. L.B.R. Orssatto, D.N. Borg, A.J. Blazevich, R.L. Sakugawa, A.J. Shield, and G.S. Trajano, Intrinsic motoneuron excitability is reduced in soleus and tibialis anterior of older adults. Geroscience 43 (2021) 2719-2735.

31. C.J. Padilla, M.E. Harrigan, H. Harris, J.M. Schwab, S.B. Rutkove, M.M. Rich, B.C. Clark, and W.D. Arnold, Profiling age-related muscle weakness and wasting: neuromuscular junction transmission as a driver of age-related physical decline. Geroscience 43 (2021) 1265-1281.

32. P. Aagaard, C. Suetta, P. Caserotti, S.P. Magnusson, and M. Kjaer, Role of the nervous system in sarcopenia and muscle atrophy with aging: strength training as a countermeasure. Scand J Med Sci Sports 20 (2010) 49-64.

33. S.S. Rudrappa, D.J. Wilkinson, P.L. Greenhaff, K. Smith, I. Idris, and P.J. Atherton, Human Skeletal Muscle Disuse Atrophy: Effects on Muscle Protein Synthesis, Breakdown, and Insulin Resistance—A Qualitative Review. Frontiers in Physiology 7 (2016).

34. M. Tomonaga, Histochemical and ultrastructural changes in senile human skeletal muscle. J. Am. Geriatr. Soc. 25 (1977) 125-131.

35. F.G. Jennekens, B.E. Tomlinson, and J.N. Walton, Histochemical aspects of five limb muscles in old age. An autopsy study. J Neurol Sci 14 (1971) 259-76.

36. G. Oertel, Changes in human skeletal muscles due to ageing. Acta Neuropathologica 69 (1986) 309-313.

37. R. Scelsi, C. Marchetti, and P. Poggi, Histochemical and ultrastructural aspects of m. vastus lateralis in sedentary old people (age 65--89 years). Acta Neuropathol 51 (1980) 99-105.

38. J. Lexell, and D. Downham, What is the effect of ageing on type 2 muscle fibres? J Neurol Sci 107 (1992) 250-1.

39. J. Lexell, D. Downham, and M. Sjostrom, Distribution of different fibre types in human skeletal muscles. A statistical and computational model for the study of fibre type grouping and early diagnosis of skeletal muscle fibre denervation and reinnervation. J Neurol Sci 61 (1983) 301-14.

40. J. Lexell, K. Henriksson-Larsen, B. Winblad, and M. Sjostrom, Distribution of different fiber types in human skeletal muscles: effects of aging studied in whole muscle cross sections. Muscle Nerve 6 (1983) 588-95.

41. J. Lexell, C.C. Taylor, and M. Sjostrom, What is the cause of the ageing atrophy? Total number, size and proportion of different fiber types studied in whole vastus lateralis muscle from 15- to 83-year-old men. J Neurol Sci 84 (1988) 275-94.

42. M. Venturelli, C. Reggiani, R.S. Richardson, and F. Schena, Skeletal Muscle Function in the Oldest-Old: The Role of Intrinsic and Extrinsic Factors. Exerc Sport Sci Rev 46 (2018) 188-194.

43. S.L. Rowan, F.M. Purves-Smith, N.M. Solbak, and R.T. Hepple, Accumulation of severely atrophic myofibers marks the acceleration of sarcopenia in slow and fast twitch muscles. Exp Gerontol 46 (2011) 660-9.

44. F. Kadi, N. Charifi, C. Denis, and J. Lexell, Satellite cells and myonuclei in young and elderly women and men. Muscle Nerve 29 (2004) 120-7.

45. I. Franco, R. Fernandez-Gonzalo, P. Vrtačnik, T.R. Lundberg, M. Eriksson, and T. Gustafsson, Healthy skeletal muscle aging: The role of satellite cells, somatic mutations and exercise. Int Rev Cell Mol Biol 346 (2019) 157-200.

46. Z. Ling, X. Liu, Y. Cheng, X. Yan, and S. Wu, Gut microbiota and aging. Critical Reviews in Food Science and Nutrition (2020) 1-56.

47. S.W. Baran, M.A. Lim, J.P. Do, P. Stolyar, M.D. Rabe, L.R. Schaevitz, and S.M. Cadena, Digital biomarkers enable automated, longitudinal monitoring in a mouse model of aging. J Gerontol A Biol Sci Med Sci (2021).

48. K. Pernold, E. Rullman, and B. Ulfhake, Major oscillations in spontaneous home-cage activity in C57BL/6 mice housed under constant conditions. Sci Rep 11 (2021) 4961.

49. L. Dohnalová, P. Lundgren, J.R.E. Carty, N. Goldstein, S.L. Wenski, P. Nanudorn, S. Thiengmag, K.-P. Huang, L. Litichevskiy, H.C. Descamps, K. Chellappa, A. Glassman, S. Kessler, J. Kim, T.O. Cox, O. Dmitrieva-Posocco, A.C. Wong, E.L. Allman, S. Ghosh, N. Sharma, K. Sengupta, B. Cornes, N. Dean, G.A. Churchill, T.S. Khurana, M.A. Sellmyer, G.A. FitzGerald, A.D. Patterson, J.A. Baur, A.L. Alhadeff, E.J.N. Helfrich, M. Levy, J.N. Betley, and C.A. Thaiss, A microbiome-dependent gut–brain pathway regulates motivation for exercise. Nature (2022).

50. T. Taetzsch, and G. Valdez, NMJ maintenance and repair in aging. Curr Opin Physiol 4 (2018) 57-64.

51. H. Johnson, K. Mossberg, U. Arvidsson, F. Piehl, T. Hökfelt, and B. Ulfhake, Increase in alpha-CGRP and GAP-43 in aged motoneurons: A study of peptides, growth factors, and ChAT mRNA in the lumbar spinal cord of senescent rats with symptoms of hindlimb incapacities. J. Comp. Neurol. 359 (1995) 69-89.

52. T.G. Graber, J.H. Kim, R.W. Grange, L.K. McLoon, and L.V. Thompson, C57BL/6 life span study: age-related declines in muscle power production and contractile velocity. Age (Dordr) 37 (2015) 9773.

53. G.A. Power, M.D. Allen, K.J. Gilmore, D.W. Stashuk, T.J. Doherty, R.T. Hepple, T. Taivassalo, and C.L. Rice, Motor unit number and transmission stability in octogenarian world class athletes: Can age-related deficits be outrun? J Appl Physiol (1985) 121 (2016) 1013-1020.

54. S. Aare, S. Spendiff, M. Vuda, D. Elkrief, A. Perez, Q. Wu, D. Mayaki, S.N. Hussain, S. Hettwer, and R.T. Hepple, Failed reinnervation in aging skeletal muscle. Skelet Muscle 6 (2016) 29.

55. M. Piasecki, A. Ireland, D.A. Jones, and J.S. McPhee, Age-dependent motor unit remodelling in human limb muscles. Biogerontology 17 (2016) 485-96.

56. M. Piasecki, A. Ireland, J. Coulson, D.W. Stashuk, A. Hamilton-Wright, A. Swiecicka, M.K. Rutter, J.S. McPhee, and D.A. Jones, Motor unit number estimates and neuromuscular transmission in the tibialis anterior of master athletes: evidence that athletic older people are not spared from age-related motor unit remodeling. Physiol Rep 4 (2016).

57. M. Piasecki, A. Ireland, J. Piasecki, D.W. Stashuk, A. Swiecicka, M.K. Rutter, D.A. Jones, and J.S. McPhee, Failure to expand the motor unit size to compensate for declining motor unit numbers distinguishes sarcopenic from non-sarcopenic older men. J Physiol 596 (2018) 1627-1637.

58. E.A. Nunes, T. Stokes, J. McKendry, B.S. Currier, and S.M. Phillips, Disuse-induced skeletal muscle atrophy in disease and nondisease states in humans: mechanisms, prevention, and recovery strategies. American Journal of Physiology-Cell Physiology 322 (2022) C1068-C1084.

59. V. Moiseeva, A. Cisneros, V. Sica, O. Deryagin, Y. Lai, S. Jung, E. Andrés, J. An, J. Segalés, L. Ortet, V. Lukesova, G. Volpe, A. Benguria, A. Dopazo, S. Aznar-Benitah, Y. Urano, A. del Sol, M.A. Esteban, Y. Ohkawa, A.L. Serrano, E. Perdiguero, and P. Muñoz-Cánoves, Senescence atlas reveals an aged-like inflamed niche that blunts muscle regeneration. Nature (2022).

60. L.C. Hunt, F.A. Graca, V. Pagala, Y.D. Wang, Y. Li, Z.F. Yuan, Y. Fan, M. Labelle, J. Peng, and F. Demontis, Integrated genomic and proteomic analyses identify stimulus-dependent molecular changes associated with distinct modes of skeletal muscle atrophy. Cell Rep 37 (2021) 109971.

61. L.A. Tintignac, H.R. Brenner, and M.A. Ruegg, Mechanisms Regulating Neuromuscular Junction Development and Function and Causes of Muscle Wasting. Physiol Rev 95 (2015) 809-52.

62. A. Pannerec, M. Springer, E. Migliavacca, A. Ireland, M. Piasecki, S. Karaz, G. Jacot, S. Metairon, E. Danenberg, F. Raymond, P. Descombes, J.S. McPhee, and J.N. Feige, A robust neuromuscular system protects rat and human skeletal muscle from sarcopenia. Aging (Albany NY) 8 (2016) 712-29.

63. R. Hennig, and T. Lomo, Firing patterns of motor units in normal rats. Nature 314 (1985) 164-6.

64. M. Altun, E. Bergman, E. Edstrom, H. Johnson, and B. Ulfhake, Behavioral impairments of the aging rat. Physiol Behav 92 (2007) 911-23.

65. M. Altun, E. Bergman, E. Edström, H. Johnson, and B. Ulfhake, Behavioral impairments of the aging rat. Physiol Behav 92 (2007) 911-23.

66. M. Grönholdt-Klein, M. Altun, M. Becklén, E. Dickman Kahm, A. Fahlström, E. Rullman, and B. Ulfhake, Muscle atrophy and regeneration associated with behavioural loss and recovery of function after sciatic nerve crush. Acta Physiol (Oxf) 227 (2019) e13335.

67. F.G. Jennekens, B.E. Tomlinson, and J.N. Walton, Data on the distribution of fibre types in five human limb muscles. An autopsy study. J. Neurol. Sci. 14 (1971) 245-257.

68. L.T. Li, G. Jiang, Q. Chen, and J.N. Zheng, Ki67 is a promising molecular target in the diagnosis of cancer (review). Mol Med Rep 11 (2015) 1566-72.

69. M. Altun, H.C. Besche, H.S. Overkleeft, R. Piccirillo, M.J. Edelmann, B.M. Kessler, A.L. Goldberg, and B. Ulfhake, Muscle wasting in aged, sarcopenic rats is associated with enhanced activity of the ubiquitin proteasome pathway. J Biol Chem 285 (2010) 39597-608.

70. E. Edstrom, M. Altun, M. Hagglund, and B. Ulfhake, Atrogin-1/MAFbx and MuRF1 are downregulated in aging-related loss of skeletal muscle. J Gerontol A Biol Sci Med Sci 61 (2006) 663-74.

71. E. Skoglund, M. Grönholdt-Klein, E. Rullman, L.E. Thornell, A. Strömberg, A. Hedman, T. Cederholm, B. Ulfhake, and T. Gustafsson, Longitudinal Muscle and Myocellular Changes in Community-Dwelling Men Over Two Decades of Successful Aging-The ULSAM Cohort Revisited. J Gerontol A Biol Sci Med Sci 75 (2020) 654-663.

72. M. Altun, E. Edstrom, E. Spooner, A. Flores-Moralez, E. Bergman, P. Tollet-Egnell, G. Norstedt, B.M. Kessler, and B. Ulfhake, Iron load and redox stress in skeletal muscle of aged rats. Muscle Nerve 36 (2007) 223-233.

73. A. Ishihara, K. Itoh, M. Itoh, C. Hirofuji, and H. Hayashi, Effects of hypophysectomy on soleus muscle fibers and spinal motoneurons in rats. Acta Neuropathol 89 (1995) 204-8.

74. A. Fahlstrom, H. Zeberg, and B. Ulfhake, Changes in behaviors of male C57BL/6J mice across adult life span and effects of dietary restriction. Age (Dordr) (2011).

75. W.N. Bair, M. Petr, I. Alfaras, S.J. Mitchell, M. Bernier, L. Ferrucci, S.A. Studenski, and R. De Cabo, Of Aging Mice and Men: Gait Speed Decline Is a Translatable Trait, With Species-Specific Underlying Properties. J Gerontol A Biol Sci Med Sci 74 (2019) 1413-1416.

76. M.A. Egerman, and D.J. Glass, Signaling pathways controlling skeletal muscle mass. Crit Rev Biochem Mol Biol 49 (2014) 59-68.

77. C. Ibebunjo, J.M. Chick, T. Kendall, J.K. Eash, C. Li, Y. Zhang, C. Vickers, Z. Wu, B.A. Clarke, J. Shi, J. Cruz, B. Fournier, S. Brachat, S. Gutzwiller, Q. Ma, J. Markovits, M. Broome, M. Steinkrauss, E. Skuba, J.R. Galarneau, S.P. Gygi, and D.J. Glass, Genomic and proteomic profiling reveals reduced mitochondrial function and disruption of the neuromuscular junction driving rat sarcopenia. Mol Cell Biol 33 (2013) 194-212.

78. L. Broom, J. Stephen, V. Nayar, and V.G. VanderHorst, Shifts in Gait Signatures Mark the End of Lifespan in Mice, With Sex Differences in Timing. Front Aging Neurosci 13 (2021) 716993.

79. D.J. Wigston, and A.W. English, Fiber-type proportions in mammalian soleus muscle during postnatal development. J Neurobiol 23 (1992) 61-70.

80. M. Naruse, S. Trappe, and T.A. Trappe, Human skeletal muscle-specific atrophy with aging: a comprehensive review. J Appl Physiol (1985) 134 (2023) 900-914.

81. S. Schiaffino, A.C. Rossi, V. Smerdu, L.A. Leinwand, and C. Reggiani, Developmental myosins: expression patterns and functional significance. Skeletal Muscle 5 (2015) 22.

82. C. Soendenbroe, J.L. Andersen, and A.L. Mackey, Muscle-nerve communication and the molecular assessment of human skeletal muscle denervation with aging. Am J Physiol Cell Physiol 321 (2021) C317-c329.

83. P. Hendrickse, M. Galinska, E. Hodson-Tole, and H. Degens, An evaluation of common markers of muscle denervation in denervated young-adult and old rat gastrocnemius muscle. Exp Gerontol 106 (2018) 159-164.

84. N.R. Cashman, J. Covault, R.L. Wollman, and J.R. Sanes, Neural cell adhesion molecule in normal, denervated, and myopathic human muscle. Ann Neurol 21 (1987) 481-9.

85. A.C. Missias, G.C. Chu, B.J. Klocke, J.R. Sanes, and J.P. Merlie, Maturation of the acetylcholine receptor in skeletal muscle: regulation of the AChR gamma-to-epsilon switch. Dev Biol 179 (1996) 223-38.

86. F. Sarto, D.W. Stashuk, M.V. Franchi, E. Monti, S. Zampieri, G. Valli, G. Sirago, J. Candia, L.M. Hartnell, M. Paganini, J.S. McPhee, G. De Vito, L. Ferrucci, C. Reggiani, and M.V. Narici, Effects of short-term unloading and active recovery on human motor unit properties, neuromuscular junction transmission and transcriptomic profile. J Physiol 600 (2022) 4731-4751.

87. R. Fernandez-Gonzalo, P.A. Tesch, T.R. Lundberg, B.A. Alkner, E. Rullman, and T. Gustafsson, Three months of bed rest induce a residual transcriptomic signature resilient to resistance exercise countermeasures. Faseb j 34 (2020) 7958-7969.

88. M.A. Stocksley, S.S. Awad, C. Young, R.N. Lightowlers, H.R. Brenner, and C.R. Slater, Accumulation of Nav1 mRNAs at differentiating postsynaptic sites in rat soleus muscles. Mol Cell Neurosci 28 (2005) 694-702.

89. S.L. Rowan, K. Rygiel, F.M. Purves-Smith, N.M. Solbak, D.M. Turnbull, and R.T. Hepple, Denervation causes fiber atrophy and myosin heavy chain co-expression in senescent skeletal muscle. PLoS One 7 (2012) e29082.

90. F. Rannou, J.P. Pennec, J. Morel, G. Guéret, R. Leschiera, M. Droguet, M. Gioux, and M.A. Giroux-Metges, Na v1.4 and Na v1.5 are modulated differently during muscle immobilization and contractile phenotype conversion. J Appl Physiol (1985) 111 (2011) 495-507.

91. J.F. Desaphy, S. Pierno, C. Léoty, A.L. George, Jr., A. De Luca, and D.C. Camerino, Skeletal muscle disuse induces fibre type-dependent enhancement of Na(+) channel expression. Brain 124 (2001) 1100-13.

92. E. Skoglund, M. Gronholdt-Klein, E. Rullman, L.E. Thornell, A. Stromberg, A. Hedman, T. Cederholm, B. Ulfhake, and T. Gustafsson, Longitudinal Muscle and Myocellular Changes in Community-Dwelling Men Over Two Decades of Successful Aging-The ULSAM Cohort Revisited. J Gerontol A Biol Sci Med Sci (2019).

93. Y. Oishi, T. Ogata, K.I. Yamamoto, M. Terada, T. Ohira, Y. Ohira, K. Taniguchi, and R.R. Roy, Cellular adaptations in soleus muscle during recovery after hindlimb unloading. Acta Physiol (Oxf) 192 (2008) 381-95.

94. A.J. Buller, J.C. Eccles, and R.M. Eccles, Interactions between motoneurones and muscles in respect of the characteristic speeds of their responses. J Physiol 150 (1960) 417-39.

95. J. Lexell, and D.Y. Downham, The occurrence of fibre-type grouping in healthy human muscle: a quantitative study of cross-sections of whole vastus lateralis from men between 15 and 83 years. Acta Neuropathol 81 (1991) 377-81.

96. J. Lexell, D. Downham, and M. Sjostrom, Distribution of different fibre types in human skeletal muscles. Fibre type arrangement in m. vastus lateralis from three groups of healthy men between 15 and 83 years. J Neurol Sci 72 (1986) 211-22.

97. G.A.M. Messa, M. Piasecki, J. Rittweger, J.S. McPhee, E. Koltai, Z. Radak, B. Simunic, A. Heinonen, H. Suominen, M.T. Korhonen, and H. Degens, Absence of an aging-related increase in fiber type grouping in athletes and non-athletes. Scand J Med Sci Sports 30 (2020) 2057-2069.

98. J.A. Baur, D. Chen, E.N. Chini, K. Chua, H.Y. Cohen, R. de Cabo, C. Deng, S. Dimmeler, D. Gius, L.P. Guarente, S.L. Helfand, S. Imai, H. Itoh, T. Kadowaki, D. Koya, C. Leeuwenburgh, M. McBurney, Y. Nabeshima, C. Neri, P. Oberdoerffer, R.G. Pestell, B. Rogina, J. Sadoshima, V. Sartorelli, M. Serrano, D.A. Sinclair, C. Steegborn, M. Tatar, H.A. Tissenbaum, Q. Tong, K. Tsubota, A. Vaquero, and E. Verdin, Dietary restriction: standing up for sirtuins. Science 329 (2010) 1012-3; author reply 1013-4.

99. J.F. Desaphy, S. Pierno, A. Liantonio, A. De Luca, M.P. Didonna, A. Frigeri, G.P. Nicchia, M. Svelto, C. Camerino, A. Zallone, and D.C. Camerino, Recovery of the soleus muscle after short- and long-term disuse induced by hindlimb unloading: effects on the electrical properties and myosin heavy chain profile. Neurobiol Dis 18 (2005) 356-65.

100. N.A. Kelly, K.G. Hammond, M.J. Stec, C.S. Bickel, S.T. Windham, S.C. Tuggle, and M.M. Bamman, Quantification and characterization of grouped type I myofibers in human aging. Muscle Nerve 57 (2018) E52-e59.

101. X. Zhou, J.L. Wang, J. Lu, Y. Song, K.S. Kwak, Q. Jiao, R. Rosenfeld, Q. Chen, T. Boone, W.S. Simonet, D.L. Lacey, A.L. Goldberg, and H.Q. Han, Reversal of cancer cachexia and muscle wasting by ActRIIB antagonism leads to prolonged survival. Cell 142 (2010) 531-43.

102. J. Zhao, J.J. Brault, A. Schild, and A.L. Goldberg, Coordinate activation of autophagy and the proteasome pathway by FoxO transcription factor. Autophagy 4 (2008) 378-80.

103. J.M. Sacheck, J.P. Hyatt, A. Raffaello, R.T. Jagoe, R.R. Roy, V.R. Edgerton, S.H. Lecker, and A.L. Goldberg, Rapid disuse and denervation atrophy involve transcriptional changes similar to those of muscle wasting during systemic diseases. FASEB J 21 (2007) 140-55.

104. S.H. Lecker, R.T. Jagoe, A. Gilbert, M. Gomes, V. Baracos, J. Bailey, S.R. Price, W.E. Mitch, and A.L. Goldberg, Multiple types of skeletal muscle atrophy involve a common program of changes in gene expression. Faseb J 18 (2004) 39-51.

105. B.A. Clarke, D. Drujan, M.S. Willis, L.O. Murphy, R.A. Corpina, E. Burova, S.V. Rakhilin, T.N. Stitt, C. Patterson, E. Latres, and D.J. Glass, The E3 Ligase MuRF1 degrades myosin heavy chain protein in dexamethasone-treated skeletal muscle. Cell Metab 6 (2007) 376-85.

106. D.J. Glass, Skeletal muscle hypertrophy and atrophy signaling pathways. Int J Biochem Cell Biol 37 (2005) 1974-84.

107. H.H. Chen, L.K. Tsai, K.Y. Liao, T.C. Wu, Y.H. Huang, Y.C. Huang, S.W. Chang, P.Y. Wang, Y.P. Tsao, and S.L. Chen, Muscle-restricted nuclear receptor interaction protein knockout causes motor neuron degeneration through down-regulation of myogenin at the neuromuscular junction. J Cachexia Sarcopenia Muscle 9 (2018) 771-785.

108. C.J. McNeil, T.J. Doherty, D.W. Stashuk, and C.L. Rice, Motor unit number estimates in the tibialis anterior muscle of young, old, and very old men. Muscle Nerve 31 (2005) 461-7.

109. M. Kawabuchi, H. Tan, and S. Wang, Age affects reciprocal cellular interactions in neuromuscular synapses following peripheral nerve injury. Ageing Res Rev 10 (2011) 43-53.

110. M. Kawabuchi, C. Zhou, K. Nakamura, and K. Hirata, Morphological features of collateral innervation and supernumerary innervation in the skeletal muscles of presenile rats. Anatomischer Anzeiger 177 (1995) 251-65.

111. M. Kawabuchi, C.J. Zhou, S. Wang, K. Nakamura, W.T. Liu, and K. Hirata, The spatiotemporal relationship among Schwann cells, axons and postsynaptic acetylcholine receptor regions during muscle reinnervation in aged rats. Anat Rec 264 (2001) 183-202.

112. A. Pestronk, D.B. Drachman, and J.W. Griffin, Effects of aging on nerve sprouting and regeneration. Experimental Neurology 70 (1980) 65-82.

113. G. Klöppel, A. Perren, and P.U. Heitz, The gastroenteropancreatic neuroendocrine cell system and its tumors: the WHO classification. Ann N Y Acad Sci 1014 (2004) 13-27.

114. Y. Cao, Z. Yao, D. Sarkar, M. Lawrence, G.J. Sanchez, M.H. Parker, K.L. MacQuarrie, J. Davison, M.T. Morgan, W.L. Ruzzo, R.C. Gentleman, and S.J. Tapscott, Genome-wide MyoD binding in skeletal muscle cells: a potential for broad cellular reprogramming. Dev Cell 18 (2010) 662-74.

115. S. Bhatnagar, A. Kumar, D.Y. Makonchuk, H. Li, and A. Kumar, Transforming growth factor-beta-activated kinase 1 is an essential regulator of myogenic differentiation. J Biol Chem 285 (2010) 6401-11.

116. P.C. Macpherson, X. Wang, and D. Goldman, Myogenin regulates denervation-dependent muscle atrophy in mouse soleus muscle. J Cell Biochem 112 (2011) 2149-59.

117. V. Moresi, A.H. Williams, E. Meadows, J.M. Flynn, M.J. Potthoff, J. McAnally, J.M. Shelton, J. Backs, W.H. Klein, J.A. Richardson, R. Bassel-Duby, and E.N. Olson, Myogenin and class II HDACs control neurogenic muscle atrophy by inducing E3 ubiquitin ligases. Cell 143 (2010) 35-45.

118. P. Hu, K.G. Geles, J.H. Paik, R.A. DePinho, and R. Tjian, Codependent activators direct myoblast-specific MyoD transcription. Dev Cell 15 (2008) 534-46.

119. R. Wiberg, S. Jonsson, L.N. Novikova, and P.J. Kingham, Investigation of the Expression of Myogenic Transcription Factors, microRNAs and Muscle-Specific E3 Ubiquitin Ligases in the Medial Gastrocnemius and Soleus Muscles following Peripheral Nerve Injury. PLoS One 10 (2015) e0142699.

120. F.M. Purves-Smith, N.M. Solbak, S.L. Rowan, and R.T. Hepple, Severe atrophy of slow myofibers in aging muscle is concealed by myosin heavy chain co-expression. Exp Gerontol 47 (2012) 913-8.

121. M. Altun, Grönholdt-Klein, M., Wang, L. and Ulfhake, B., Cellular Degradation Machineries in Age-Related Loss of Muscle Mass (Sarcopenia). in: T. Nagata, (Ed.), Senescence, InTech, 2012, pp. 269-286.

122. L.B. Verdijk, R. Koopman, G. Schaart, K. Meijer, H.H. Savelberg, and L.J. van Loon, Satellite cell content is specifically reduced in type II skeletal muscle fibers in the elderly. Am J Physiol Endocrinol Metab 292 (2007) E151-7.

123. L.B. Verdijk, T. Snijders, M. Drost, T. Delhaas, F. Kadi, and L.J. van Loon, Satellite cells in human skeletal muscle; from birth to old age. Age (Dordr) 36 (2014) 545-7.

124. Y. Ming, E. Bergman, E. Edström, and B. Ulfhake, Evidence for increased GDNF signaling in aged sensory and motor neurons. NeuroReport 10 (1999) 1529-1535.

125. E. Bergman, S. Kullberg, Y. Ming, and B. Ulfhake, Upregulation of GFRalpha-1 and c-ret in primary sensory neurons and spinal motoneurons of aged rats. J. Neurosci. Res. 57 (1999) 153-165.

126. S. Stanga, M. Boido, and P. Kienlen-Campard, How to Build and to Protect the Neuromuscular Junction: The Role of the Glial Cell Line-Derived Neurotrophic Factor. Int J Mol Sci 22 (2020).

127. M. Hollyday, and V. Hamburger, Reduction of the naturally occurring motor neuron loss by enlargement of the periphery. J Comp Neurol 170 (1976) 311-20.

128. R.W. Oppenheim, Neurotrophic survival molecules for motoneurons: an embarrassment of riches. Neuron 17 (1996) 195-197.

129. F. Rieger, M. Nicolet, M. Pinçon-Raymond, M. Murawsky, G. Levi, and G.M. Edelman, Distribution and role in regeneration of N-CAM in the basal laminae of muscle and Schwann cells. J Cell Biol 107 (1988) 707-19.

130. R. Csapo, M. Gumpenberger, and B. Wessner, Skeletal Muscle Extracellular Matrix - What Do We Know About Its Composition, Regulation, and Physiological Roles? A Narrative Review. Front Physiol 11 (2020) 253.

131. H.L. Birch, Extracellular Matrix and Ageing. Subcell Biochem 90 (2018) 169-190.

132. M.V. Plikus, X. Wang, S. Sinha, E. Forte, S.M. Thompson, E.L. Herzog, R.R. Driskell, N. Rosenthal, J. Biernaskie, and V. Horsley, Fibroblasts: Origins, definitions, and functions in health and disease. Cell 184 (2021) 3852-3872.

133. A. Martin, and D. Freyssenet, Phenotypic features of cancer cachexia-related loss of skeletal muscle mass and function: lessons from human and animal studies. J Cachexia Sarcopenia Muscle 12 (2021) 252-273.

134. C. Sherrington, N.J. Fairhall, G.K. Wallbank, A. Tiedemann, Z.A. Michaleff, K. Howard, L. Clemson, S. Hopewell, and S.E. Lamb, Exercise for preventing falls in older people living in the community. Cochrane Database Syst Rev 1 (2019) Cd012424.

135. L.F. Ferreira, E.L. Scariot, and L.H.T. da Rosa, The effect of different exercise programs on sarcopenia criteria in older people: A systematic review of systematic reviews with meta-analysis. Arch Gerontol Geriatr 105 (2023) 104868.

136. M.A. Fiatarone, E.C. Marks, N.D. Ryan, C.N. Meredith, L.A. Lipsitz, and W.J. Evans, High-intensity strength training in nonagenarians. Effects on skeletal muscle. Jama 263 (1990) 3029-34.

137. R.H. Whipple, L.I. Wolfson, and P.M. Amerman, The Relationship of Knee and Ankle Weakness to Falls in Nursing Home Residents: An Isokinetic Study. Journal of the American Geriatrics Society 35 (1987) 13-20.